VOLUME 21, 1959/60, No. 8 pp. 221-252 Published 30th June 1960

Philips Technical Review

DEALING WITH TECHNICAL PROBLEMS
RELATING TO THE PRODUCTS, PROCESSES AND INVESTIGATIONS OF
THE PHILIPS INDUSTRIES

REFLEX KLYSTRONS FOR WAVELENGTHS OF 4 AND 2.5 mm

by B. B. van IPEREN.

621.385.6.029.65

In recent years there have been attempts on every hand to produce shorter and shorter wavelengths, both with the familiar types of microwave tubes and also with devices operating on different principles. In this respect the reflex klystron has proved to be capable of a surprisingly good performance. A few years ago Philips were the first to bring out a reflex klystron for 4 mm waves, and now good results have also been achieved with a klystron for 2.5 mm waves.

Reflex klystrons for millimetre wavelengths are mainly used in radar receivers, in waveguide communication systems, and for various research purposes, e.g. for microwave spectroscopy and temperature measurements on gas-discharge plasma (from the propagation properties of microwaves in a plasma one can derive the electron density and temperature of the plasma). The latter application is of especial importance in that it allows the determination of the enormously high gas temperatures, of the order of millions of °K, required to initiate thermonuclear reactions.

The reflex klystron has proved to be an eminently useful type of tube for generating microwaves. Its power output is of the order of 10 to 1000 mW, which is quite adequate for many purposes. Articles on a reflex klystron for 4 mm waves appeared in this journal and elsewhere some years ago [1]). Tubes of this type are now being manufactured by Philips in small numbers and with reasonable reproducibility [2]). Some details of these are given below. We then deal with theoretical considerations concerning the production of even shorter waves, and which have led to the design of a reflex klystron for operation at about 2.5 mm wavelength. This tube, with which a wavelength as short as 2.3 mm has been achieved, and which is still in the experimental stage, will be discussed at the end of this article.

In its simplest form a reflex klystron consists of an electron gun, a resonant cavity and a repeller electrode (*fig. 1*). The electron gun "shoots" a beam of electrons through a resonant cavity which contains two central holes and also constitutes the anode. After passing through the resonant cavity, where they are modulated in velocity (by the minute oscillation already present, due to noise fluctuations or the transient resulting from switching-on the electron beam), they are returned by the repeller, which has a negative potential V_r with respect to the cathode. Provided V_r and the distance from the repeller to the cavity are properly chosen, the returning electrons again pass through the cavity in such a phase that, by interaction with the electromagnetic resonator field, they give up energy to the resonant cavity. The oscillation is thus

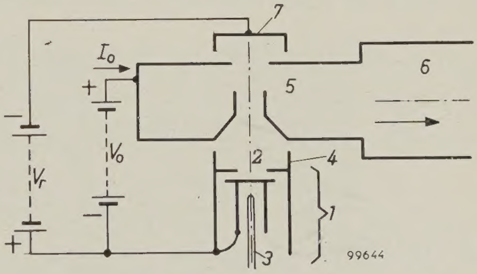

Fig. 1. Schematic axial cross-section of a reflex klystron. *1* electron gun with cathode *2*, heater *3* and focusing electrode *4*. *5* resonant cavity (also anode) with output waveguide *6*. *7* repeller electrode. V_0 accelerating voltage. I_0 beam current. V_r repeller voltage.

---

[1]) B. B. van Iperen, A reflex klystron for 4 mm waves, Philips tech. Rev. **18**, 51-52, 1956/57; Klystrons reflex pour ondes millimétriques, Le Vide 11, 264-266, 1956.

[2]) The last stage in the development of this tube was the work of H. W. van der Voorn, now in charge of its manufacture.

amplified, so that subsequent electrons are more strongly modulated in velocity and so on. The system thus acts as a generator.

If the tube is to operate at an accelerating potential V_0 lower than e.g. 1000 V, more elaborate constructions are necessary, making use of grids in the resonant cavity, or of a ribbon-shaped or hollow electron beam. Where the aim, however, is to generate oscillations of the highest possible frequency ,grids can better be dispensed with, since electron bombardment overheats them and therefore limits the maximum power per unit surface area. One may therefore expect tubes without grids to be capable of generating higher frequencies, and our investigations have accordingly been limited to this particular type. Our object being to develop tubes for continuous operation, attention had to be paid to the dissipation problem in spite of the absence of grids.

To simplify as far as possible the technological problems involved, a design with axial symmetry was adopted, using a "solid" electron beam — in principle, therefore, as illustrated schematically in fig. 1.

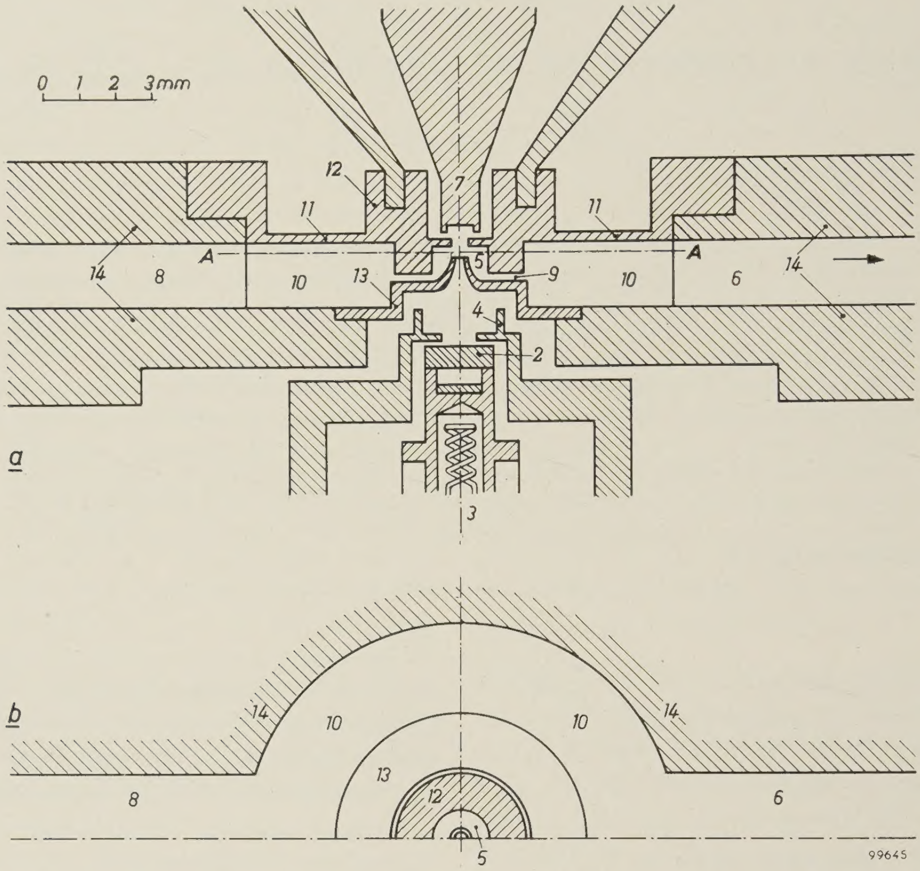

Fig. 2. Central portion of type DX 151 reflex klystron for 4 mm waves. *a*) axial section, *b*) transverse section along horizontal plane through *A*-*A* in (*a*). *2* L cathode. *3* heater. *4* focusing electrode. *5* resonant cavity. *6* output waveguide. *7* repeller. *8* waveguide with shorting plunger (not shown). *9* quarter-wave transformer. *10* annular space (*9*, *10* and *8* together form the matching transformer between the resonant cavity *5* and the output waveguide *6*). *11* thin wall allowing copper section *12* to be moved axially in relation to the copper section *13* by means of an external tuning mechanism (mechanical tuning). *14* copper block in which central portion is mounted. Dimensions:

Diameter of opening in electrode *4*	1.0 mm	Diameter of holes in *12* and *13* . .	0.25 mm
Diameter of resonant cavity *5* . .	1.6 mm	Width of waveguides *6* and *8* . .	3.6 mm
Height of resonant cavity *5* . . .	0.7 mm	Height of waveguides *6* and *8* . .	1.8 mm

The DX 151 reflex klystron for 4 mm waves

The type DX 151 reflex klystron for 4 mm waves now being manufactured is a further development of the tube dealt with in the article mentioned under footnote 1). *Fig. 2* represents a cross-section of the central portion, showing the electron gun with its components *2*, *3* and *4*, the resonant cavity *5*, the output waveguide *6* and the repeller electrode *7*. Diametrically opposite the output waveguide is a second waveguide *8*, containing a shorting plunger for adjusting the optimum load impedance. Mica windows in the waveguide provide the necessary vacuum seal. The output waveguide is coupled to the resonant cavity via a matching transformer; this consists of a gap *9* measuring about $\frac{1}{4}$ wavelength in the axial direction, an annular space *10* and the waveguide *8* with shorting plunger. One wall of the space *10* is so thin at one point (at *11*) as to enable the upper part of the tube to be moved axially in relation to the bottom part by means of an external tuning mechanism. This displacement varies the gap width of the interaction space and hence the equivalent capacitance of the resonant cavity. In this way the resonance frequency can be varied continuously over a range of about 10 to 15%, for a displacement of about 100 μ.

Because of its complexity is not possible to calculate directly the properties of the matching transformer. However, its mirror symmetry allows a simple equivalent circuit to be given, from which insight can be obtained into the operation of the shorting plunger as a matching element. In this circuit, shown in *fig. 3*, the resonant cavity is replaced by an *L-C-R* network. This is connected by a lecher line (electrical length x and characteristic impedance $2Z_0$) to two other lecher lines in series (characteristic impedance Z_0), one of which is terminated by the load (ordinarily with impedance Z_0) and the other by a sliding shorting bridge corresponding to the plunger. When this bridge is positioned such that the distance to the branching point is $2n+1)\lambda/4$, where n is a whole number, the load conductance measured across the circuit is zero, indicating that the load is entirely decoupled from the resonant cavity. This means that the load can be reduced to any desired value by moving the bridge. In tubes for mm waves this is a very desirable feature, particularly where the object is to achieve the shortest possible wavelength.

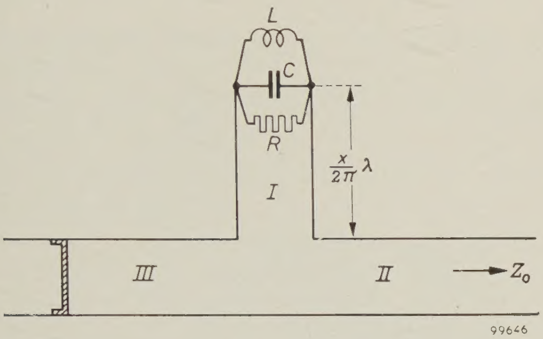

Fig. 3. Equivalent circuit of matching transformer *9-10-8* in fig. 2. *L-C-R* represents the resonant cavity *5*. *I* is a lecher line with characteristic impedance $2Z_0$ and electrical length x; *II* and *III* are lecher lines of characteristic impedance Z_0, replacing waveguides *6* and *8*, respectively.

The maximum load conductance obtainable depends on x and Z_0. In practice the tendency is to design the matching transformer in such a way that x and Z_0 in the required frequency band have values that make it possible to vary the load over a sufficiently wide range.

Fig. 2 also shows some constructional details. The waveguides *6* and *8*, the annular space *10* and the place for the copper sections *12* and *13*, which together constitute the resonant cavity and the $\frac{1}{4}$-wave transformer, are cut in a single block of copper *14*. Parts *12* and *13* are made by a hot-pressing process, the high precision of which benefits the reproducibility of the tube characteristics.

One of the most difficult technical problems in tubes of this kind is the accurate alignment of the electrodes; in the present case the alignment must be accurate to within 10 μ. This was solved satisfactorily by mounting the electron gun and the repeller in such a way that, after the tube is sealed off, they can still be moved fractionally in various directions perpendicular to the axis of the tube (after-alignment). For this purpose a flexible diaphragm is used as part of the tube wall. *Fig. 4* shows the arrangement in the case of the repeller; a similar arrangement is adopted for the electron gun.

For reasons explained below, a very high current density is required from the cathode in such tubes. This makes the use of a dispenser-type cathode, e.g. an L cathode [3]), essential. Moreover, the L cathode readily fulfils another condition, namely that the emitting surface must be smooth to within about 1 μ in order for the electron beam to have the correct shape. The L cathode used in the DX 151 tube delivers the required current density of 2.5 A/cm² for an average useful life of several thousands of hours.

The diameter of the electron beam at the narrowest point is about 0.12 mm, i.e. roughly half the diameter of the holes in the resonant cavity. A beam as narrow as this is required in order that the majority of the electrons will still pass through the resonant cavity in spite of the beam having widened out in its passage to and fro in the repeller space.

Fig. 5 shows the output power (the average over several tubes) as a function of frequency and wavelength. A photograph of the tube, complete with

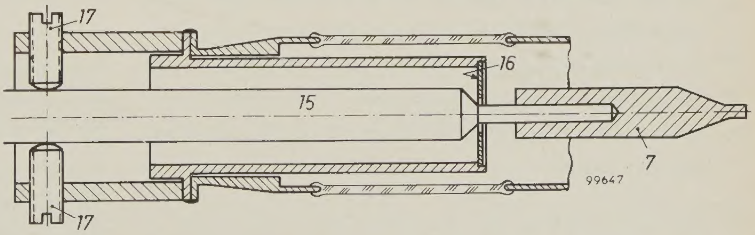

Fig. 4. The repeller electrode *7* is fitted to a stem *15*: this is fixed vacuum-tight in a flexible diaphragm *16*. By adjusting screws *17* the alignment of the repeller in relation to the axis of the stem can be altered whilst the tube is operating. Two other screws permit adjustment in a direction at right-angles to the first. The same system is used for after-alignment of the electron gun.

---

[3]) H. J. Lemmens, M. J. Jansen and R. Loosjes, A new thermionic cathode for heavy loads, Philips tech. Rev. **11**, 341-350, 1949/50.

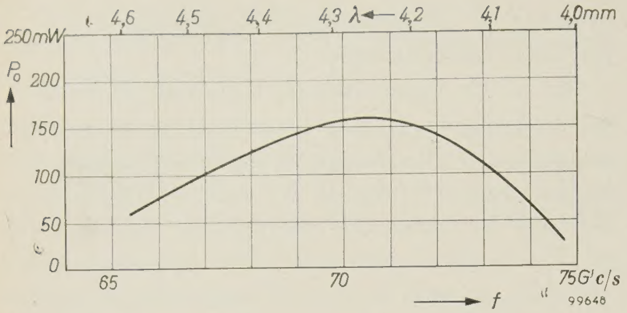

Fig. 5. Power output P_0 of type DX 151 reflex klystron (average value over several tubes) as a function of frequency f (in Gc/s = 10^9 c/s) and wavelength λ, varied by the tuning mechanism. The repeller voltage was adjusted to the most favourable value for each measurement.

tuning mechanism and further accessories, can be seen in *fig. 6*: the principal electrical data are given in the caption.

Possibilities of generating even shorter waves

The results obtained with the 4 mm klystron prompted a theoretical investigation into the possibilities of generating even shorter waves with tubes of the same kind. In this connection it is useful first of all to compare the practical results with those derived from the simple theory of reflex klystrons. According to the elementary theory the efficiency, i.e. the proportion of the D.C. power input which is converted into useful high-frequency power, is given by the formula [5]):

$$\eta = \frac{k\beta_2}{2\pi N\beta_1} X^2 J_2(X) . \quad . \; . \; . \quad (1)$$

In this expression,

k is the fraction of the original electron beam that passes through the interaction space of the resonant cavity on the way back,

N is the transit time of a non-velocity-modulated electron in the repeller space, expressed in terms of the period of the high-frequency voltage (N is a whole number $+ \frac{3}{4}$),

β_1 is the coupling factor of the forward beam with the resonant cavity, and

β_2 is the coupling factor of the returning beam with the cavity (for explanation see below),

X is the bunching parameter (this term will also be explained presently), and

J_2 is the Bessel function of the first kind and the second order.

The meaning of the coupling factors β_1 and β_2 is most readily understood in the case of velocity modulation by means of two grids between which there is an alternating voltage $\tilde{V}\cos 2\pi t/T$. An electron passing between this pair of grids in a time which is very small compared with the period T undergoes a change in kinetic energy equal to $e\tilde{V}\cos 2\pi t_M/T$, where t_M is the moment at which the electron is situated midway between the two grids. If the time taken to pass between the grids is not very small compared with T, a correction factor β must be applied. The value of β is independent of t_M. It can easily be seen that β is smaller than unity if we consider an electron passing through at the moment $t_M = 0$.

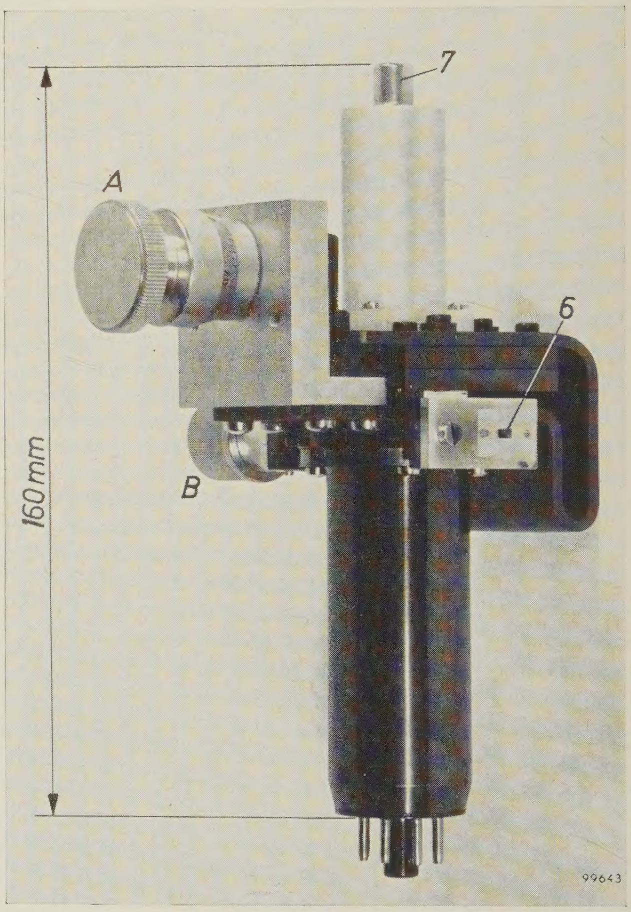

Fig. 6. Reflex klystron, type DX 151, for 4 mm waves, complete with tuning mechanism and other accessories. *6* output waveguide. *7* repeller connection. *A* tuning knob. *B* knob for adjusting shorting plunger. Principal electrical data:

Beam voltage V_0	2500 V
Beam current I_0	15-17 mA
Repeller voltage V_r	—150 to —500 V
Current density J_k at the cathode	2.4 A/cm²
Current density in the beam, in the interaction space	120 A/cm²
Power output P_0 in the middle of the frequency band	100-200 mW
Mechanical tuning range	15 %
Electronic tuning range [4])	~100 Mc/s.

---

[4]) The "electronic" tuning range is the range over which the frequency changes when V_r is varied between the two values at which the power has dropped to half its maximum value (the 3 dB points).

[5]) D. R. Hamilton, J. K. Knipp and J. B. H. Kuper, Klystrons and microwave triodes, Radiation Laboratory Series No. 7, McGraw-Hill, New York 1948, p. 311.

The bunching parameter X is equal to π times the product of the modulation depth $\tilde{V}/V_0$ and the electron transit time N. Where X is small, XI_0 (I_0 being the beam current) is exactly equal to the alternating current produced in the beam as a result of the velocity-modulation process [6]). At greater values of X saturation occurs, as a result of which the alternating current component becomes smaller than XI_0. The value which X (and hence the alternating voltage $\tilde{V}$) assumes in the oscillating tube depends not only on the tube itself but on the value of the externally applied load. For X we can write:

$$\mathrm{J}_0(X) = \frac{G_\mathrm{R} + G_\mathrm{B}}{\pi k N \beta_1 \beta_2 G_0}, \quad . \quad . \quad . \quad . \quad (2)$$

where

J_0 is a Bessel function of the first kind and zero order,

G_R is the resonance conductance of the resonant cavity,

G_B is the load conductance formed by the electron beam, and

G_0 is the D.C. conductance of the beam, i.e. I_0/V_0.

We shall first apply formulae (1) and (2) to the 4 mm klystron, type DX 151. The approximate relevant data for this type are: $k = 0.8$, $\beta_1 = 0.36$, $\beta_2 = 0.47$ and $N \approx 7$, hence $\pi k N \beta_1 \beta_2 \approx 3$. Taking into account that the resonant cavity rises to an average temperature of 175 °C above room temperature, we calculate for G_R the value

$$13 \times 10^{-6}\ \mathrm{ohm}^{-1}.$$

G_B is of the order of $0.1 \times 10^{-6}\ \mathrm{ohm}^{-1}$, and is thus practically negligible compared with G_R, and where $I_0 = 15$ mA we have

$$G_0 = \frac{15\ \mathrm{mA}}{2500\ \mathrm{V}} = 6 \times 10^{-6}\ \mathrm{ohm}^{-1}.$$

From (2) we now find

$$\mathrm{J}_0(X) = \frac{13 \times 10^{-6}}{3 \times 6 \times 10^{-6}} = 0.72.$$

The corresponding value of X substituted in (1) then gives $\eta = 0.5\%$. At a power consumption of 15 mA × 2500 V = 37.5 W, this corresponds to an output of about 200 mW, and with the best of the fabricated tubes this value is in fact achieved.

To produce a tube for still shorter wavelengths, the obvious thing to do is to scale down the dimensions in proportion to the wavelength. At this juncture we shall disregard the technical difficulties and increased dissipation per unit surface area which this involves. Scaling-down does not affect the quantities occurring in (1) and (2), with the exception of G_R, which increases proportionally with the root of the frequency. Taking the DX 151 as the tube to be scaled down, we find that for a given reduction factor the numerator of (2) becomes equal to the denominator, in which case $\mathrm{J}_0(X) = 1$ and therefore $X = 0$. According to (1) the efficiency is then zero, that is to say, the tube no longer oscillates. The minimum wavelength at which this is the case is found to be 1.5 mm.

There are various reasons why this theoretical minimum wavelength cannot be achieved in practice. One possible reason, heat dissipation, has been mentioned above: the tube gets excessively hot if the surface area becomes too small. Another reason may be electrical breakdown, owing to insufficient clearance between the parts carrying the accelerating potential (in the DX 151 there is a potential of 3000 V between points only 0.17 mm apart!).

A third reason is that, at $\lambda = 1.5$ mm, the current density J_k at the cathode is greater than any known cathode is capable of delivering under conditions of space-charge limitation. The result of scaling-down is to decrease the surface area of the cathode in proportion to λ^2, although the current I_0 remains constant. Taking 4.3 mm as the average optimum wavelength of the DX 151, and $J_\mathrm{k} = 2.4\ \mathrm{A/cm^2}$, which is the value of the current density for this tube, we find for J_k at $\lambda = 1.5$ mm:

$$\left(\frac{4.3}{1.5}\right)^2 \times 2.4 = 20\ \mathrm{A/cm^2}.$$

A good L cathode cannot be expected to give more than 8 A/cm², so that as far as the cathode is concerned the minimum wavelength is

$$\sqrt{\frac{2.4}{8}} \times 4.3 = 2.4\ \mathrm{mm}.$$

It might be asked whether a modified design would not make it possible to generate waves shorter than 2.4 mm without the current density on the cathode having to be greater than 8 A/cm². Such a design would in any case have to satisfy the oscillation condition. This condition, as far as the elementary theory applies, is that the right-hand side of (2) must be smaller than unity, i.e.:

$$G_\mathrm{R} + G_\mathrm{B} < \pi k N \beta_1 \beta_2 G_0. \quad . \quad . \quad . \quad (3)$$

It is thus a matter of designing a tube which, at a wavelength as short as possible, will still satisfy (3) without J_k exceeding a specified value. A complete answer to this problem cannot be given since effects are involved that do not lend themselves to theoretical treatment. With the aid of experimental data, however, an estimate can be made of the minimum wavelength obtainable with a reflex klystron (but leaving out of account such questions as heat dissipation and electrical break-down). This estimate is arrived at by determining 1) the magnitude of the starting current, i.e. the minimum beam current needed according to (3) to excite oscillations, and 2) whether this current can be achieved.

---

[6]) See Philips tech. Rev. **13**, 210, 1951/52. The product $\pi\alpha\xi$ found there is identical with the parameter X.

The first step amounts to determining the starting current as a function of wavelength, the accelerating voltage V_0 and the diameter $2b$ of the holes in the resonant cavity. The remaining parameters, i.e. the other dimensions of the resonant cavity and the transit time N in the repeller space, must have the optimum values necessary to make the starting current as small as possible. Choosing the optimum value of N may be rather difficult. The oscillation condition, according to the elementary theory, implies that the starting current should constantly decrease as N increases and should show no minimum as a function of N. This theory, however, takes no account of various effects such as debunching of the electrons under the influence of space-charge forces, as a result of which the alternating current in the beam decreases, and differences in the transit time of electrons which describe different trajectories (transit-time spread). Above a certain value of N these effects cause the starting current to increase rapidly with N. Consequently, the starting current does in fact show a definite minimum as a function of N, but its position cannot be calculated. From experimental data of a number of differently-dimensioned tubes we found the best value to be $N \approx 8$. (It might be possible to obtian a more favourable value, however, by a more efficient design of the electrodes.)

The second question was whether the required starting current I_0 can be achieved, i.e. whether the electron beam with the current I_0, and at given values of J_k and V_0, can be made so narrow in cross-section as to allow it to pass through the resonator holes whose diameters are $2b$. It appears that in the range of parameter values with which we are concerned, the cross-section of the beam at the narrowest position is governed entirely by the initial thermal velocities of the electrons. This fact is demonstrated in the case of tube DX 151: calculation, disregarding the thermal velocities, shows 7 μ to be the smallest diameter of the beam, but the result when the thermal velocities are taken into account is 125 μ. The latter value agrees with the measurements.

Fig. 7 shows the results of the calculation for tubes in which $V_0 = 2000$ V and where the cathode temperature was 1450 °K (at which the L cathode delivers its maximum current density). The solid curves represent the beam current I_0, required to excite oscillations, as a function of the radius b of the holes, with the wavelength as parameter. The dashed lines represent the maximum beam currents that can pass through a hole having a radius b, plotted as functions of b for various values of J_k.

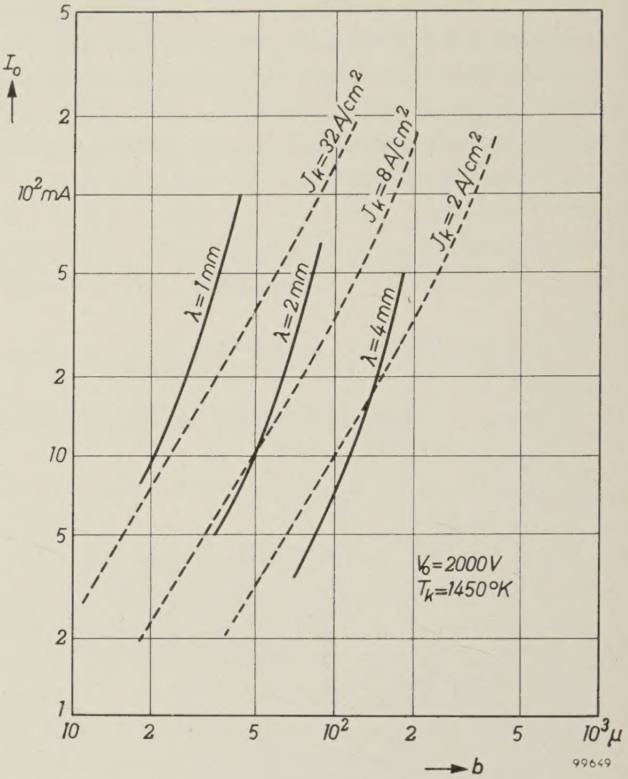

Fig. 7. Graph for calculating the minimum wavelength of reflex klystrons for $V_0 = 2000$ V, and a cathode temperature of 1450 °K. Solid curves: the calculated beam current I_0 required to excite oscillation, as a function of the radius b of the holes in the resonant cavity, for various wavelengths λ. Dashed lines: calculated maximum beam current I_0 capable of passing through a hole of radius b, as a function of b and with the current density J_k at the cathode as parameter. For $J_k = 8$ A/cm² the minimum wavelength is approximately 2 mm and the maximum value of $2b$ is 100 μ.

These calculations were confined to a Pierce electron gun. There is reason to assume, however, that other designs of gun will not yield appreciably better results. It was further assumed that the cone formed by the electron beam emerging from the gun has a semi-apex angle of $\frac{1}{3}$ radian, a value that will be difficult to exceed in tubes for wavelengths shorter than about 2 mm.

Oscillation at a given wavelength, and without J_k exceeding a specific value, can only occur at values of b for which the relevant solid curves in fig. 7 lie below the dashed curve corresponding to the permissible value of J_k. It can be seen from the figure that, at the maximum attainable emission density $J_k = 8$ A/cm^2 (and $V_0 = 2000$ V), the minimum wavelength is about 2 mm, for which the maximum permissible diameter $2b$ of the resonator holes is 100 μ. The minimum wavelength found from a similar graph for $V_0 = 4000$ V would be only slightly shorter, namely 1.6 mm. Electrical breakdown, however, would be much more difficult to avoid than at 2000 V.

A reflex klystron for 2.5 mm waves

Whether the theoretically estimated minimum wavelength can in fact be achieved depends on various circumstances already mentioned in passing, such as heat dissipation, electrical breakdown and constructional difficulties. It is not yet possible to say to what extent these problems will govern the minimum wavelength obtainable in practice. The results obtained with the tube discussed below have shown, however, that it is certainly possible to achieve a wavelength of 2.5 mm.

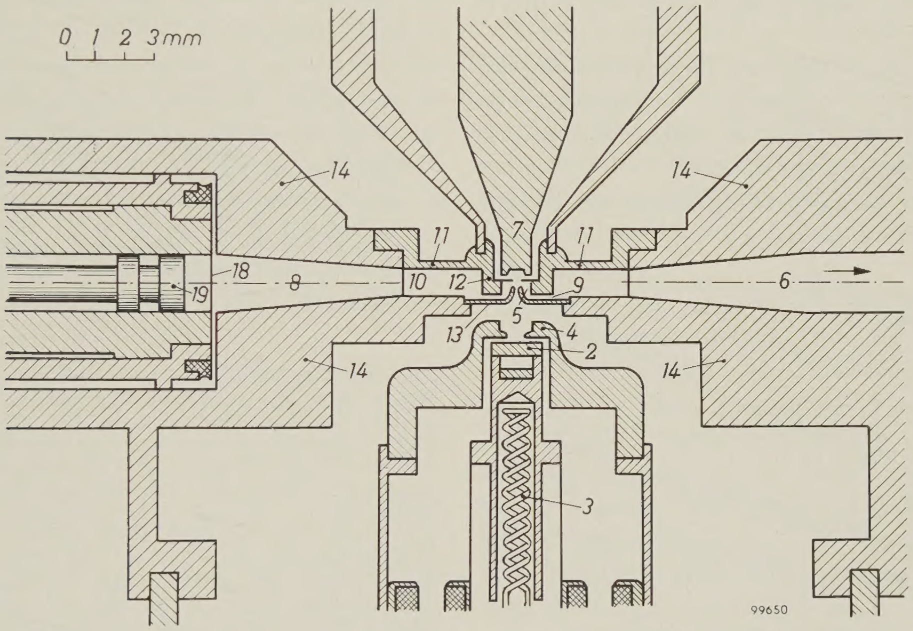

Fig. 8. Central portion of experimental reflex klystron for 2.5 mm waves, shown in axial section. Numbers *2* to *14* as in fig. 2. *18* mica window. *19* shorting plunger. Dimensions:

Diameter of opening in electrode *4*	0.6 mm	Diameter of holes in *12* and *13* .	0.15 mm
Diameter of resonant cavity *5* . .	1.0 mm	Diameter of waveguides *6* and *8* .	2.0 mm
Height of resonant cavity *5* . . .	0.4 mm		

A tube for 2.5 mm waves cannot be produced by simply scaling-down the 4 mm type, since the heat dissipation would then be inadequate, at least in continuous operation. Nevertheless it proved possible — although perhaps somewhat at the expense of the electrical properties of the matching transformer — to design a suitable tube in which the heat can be adequately dissipated. The repeller presented some difficulties, since it was not possible to reduce its distance from the resonant cavity in view of the danger of breakdown. However, with suitably modified dimensions, the repeller continued to fulfil its purpose without having to be placed nearer to the resonator.

A cross-section of the tube is shown in *fig. 8*. The waveguides are now circular instead of rectangular, thus simplifying the construction of the mica windows and plunger. One of the windows (*18*) is so close to the annular space as to make the length of the waveguide to the plunger *19* particularly small. This reduces the losses in this section of waveguide, which adversely affect the properties of the matching transformer. Here too, the electron gun and the repeller are mounted in such a way as to permit after-alignment when the tube is in operation.

The accelerating voltage is 2400 to 2500 V, the beam current 15 to 17 mA. The electron beam has a diameter of about 80 μ at its narrowest point, where the current density is slightly over 300 A/cm^2.

As with the 4 mm tube, the frequency can be varied mechanically over a range of 10 to 15% by varying the height of the resonant cavity.

Fig. 9 shows the output P_0 as a function of frequency and wavelength, measured on two experi-

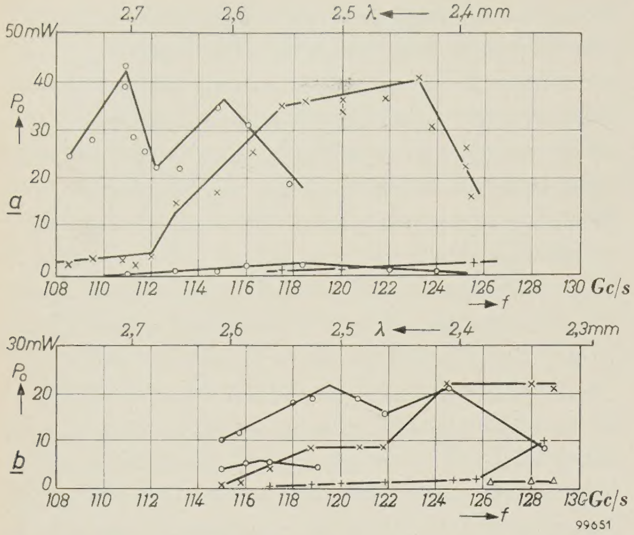

Fig. 9. Power output P_0 of two experimental reflex klystrons for 2.5 mm waves, as a function of frequency f and wavelength λ. The curves refer to various values of electron transit time N.

mental tubes. At $\lambda = 2.5$ mm an output of 40 mW was obtained; at $\lambda = 2.3$ mm — the shortest wavelength thus far generated by reflex klystrons — the measured output was 20 mW.

The curves in *fig. 10* represent the optimum repeller voltage V_r as a function of the mechanically adjusted frequency, for various values of the electron transit time N.

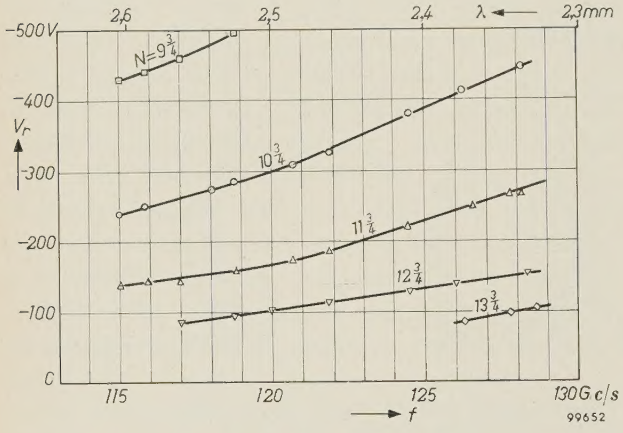

Fig. 10. The optimum repeller voltage V_r of one of the experimental 2.5 mm reflex klystrons, as a function of frequency f and wavelength λ, adjusted with the tuning mechanism. The curves relate to successive values of electron transit time N.

The output P_0 was measured by means of a bolometer employing a thermistor [7]. The thermistor was about 1 mm long, i.e. almost half a wavelength, and was mounted in a waveguide of 2 mm diameter. In spite of the relatively large dimensions of the thermistor, the error in the power measurement was calculated to be no more than a few per cent, and measurements have confirmed this. High-frequency losses occur outside the thermistor, however. The curves in fig. 9 were not corrected for these losses, and they therefore indicate the lower limit of the output.

Summary. The reflex klystron for a wavelength of 4 mm, mention of which was made some years ago, is now being manufactured in small numbers (type DX 151). It operates on 2500 V, draws a current of 15-17 mA and delivers an output of 100-200 mW. The cathode is of the dispenser type (L cathode). After a short description of this tube, the question is considered of how far it is possible to go in generating even shorter waves with reflex klystrons. If the essential dimensions of an existing tube, e.g. type DX 151, are proportionately scaled down, various difficulties are soon encountered, such as excessive current density at the cathode, inadequate heat dissipation and increased risk of electrical breakdown. With 8 A/cm^2 as the maximum current density obtainable from an L cathode, and an accelerating voltage of 2000 V, the theoretical minimum wavelength is estimated at about 2 mm. Experimental tubes have been designed along these lines for a wavelength of 2.5 mm. They operate on 2400-2500 V and 15-17 mA; the output measured at 2.5 mm is about 40 mW and at 2.3 mm about 20 mW.

---

[7] In the mm wave region a bolometer using a thermistor has special advantages. For the temperature-dependent resistor of a bolometer there is generally a choice between a thin metal wire and a thermistor. A wire, long enough to dissipate sufficient power, will not be short enough compared with the wavelength in the case of mm waves. As a result, appreciable temperature differences will occur along the wire when heated by a high-frequency current. Owing to these temperature differences the sensitivity will differ from the D.C. sensitivity for which the instrument is calibrated. On the other hand the thermistor material (ceramic semiconductor) has a so much higher ratio of thermal conductivity to electrical conductivity that, in spite of unequal heating, no appreciable temperature differences occur. In this case, then, the D.C. calibration can still be relied upon in the mm wave range.

A SIMPLE CIRCUIT FOR A LIGHT SOURCE OF CONSTANT INTENSITY

by H. van SUCHTELEN.

535.241.42:621.3.078.3:621.383.4

In many measurements employing a light source, e.g. photometric measurements of luminous intensity, and absorption measurements with a colorimeter or spectrometer, it is important that the light source should be of very constant intensity. This article describes a simple circuit in which a cadmium-sulphide photoresistor [1]) is used to keep the emission of an incandescent lamp at constant intensity.

The luminous intensity of an incandescent lamp depends closely on the applied voltage. Curve *a* in *fig. 1* shows the percentage change in the luminous intensity of a given lamp in relation to voltage variations from a nominal 220 V. A 10% voltage variation changes the luminous intensity by 34%. For the purpose of measurements these voltage variations are usually eliminated by supplying the lamp from accumulators or via an A.C. voltage stabilizer. An accumulator can deliver a sufficiently constant voltage, but it requires a great deal of attention; moreover its bulk is a disadvantage. Simple stabilizers can be designed using a transformer with a saturated core [2]). The circuit shown in *fig. 2*, for example, provides a degree of stabilization. However, as can be seen from curve *b* in fig. 1, where the alternating supply was stabilized with this circuit, it is not adequate where an incandescent lamp of really constant intensity is required.

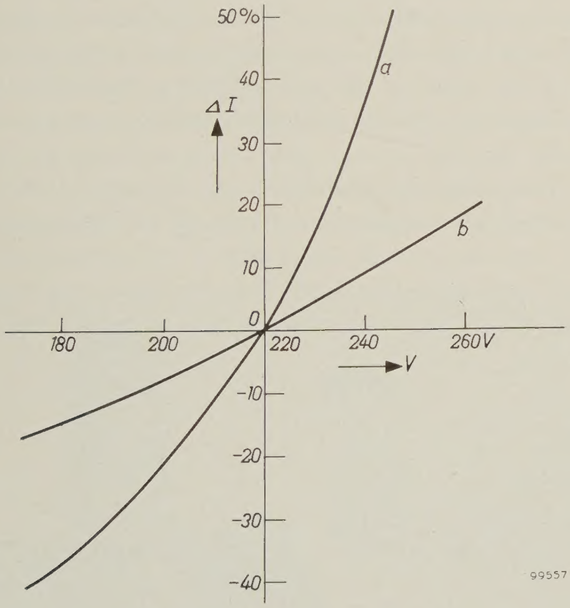

Fig. 1. Effect of mains voltage fluctuations on the luminous intensity of an incandescent lamp. The curves show the percentage change of luminous intensity in relation to the value at 220 V, *a* for a lamp without stabilizer, *b* for a lamp connected to a simple A.C. voltage stabilizer.

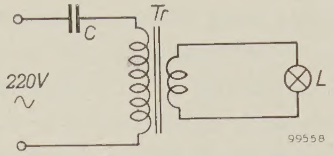

Fig. 2. Circuit of a simple mains-voltage stabilizer. *Tr* transformer with saturated core, *C* capacitor, *L* load.

Even if a better voltage stabilizer or a battery be used, however, there still remains the drawback that in the long run, the voltage being constant, the luminous intensity will decline due to the gradual evaporation of the filament and deposition on the bulb. Fundamentally, therefore, the luminous intensity *itself* should be stabilized rather than the supply voltage.

Although this can quite readily be done with an orthodox high-vacuum photocell and electron tubes, it has never found much practical application. The apparatus required is probably somewhat too complicated to be appreciated in the circles where it would be used in this case. Advances in the development of photoresistors and transistors have now made it possible, however, to design simple circuits that are eminently suited for stabilizing a small incandescent lamp of e.g. 30 watts. An experimental apparatus of this type has been built for use with a spectrometer in the Philips Research Laboratories, Eindhoven.

The circuit was designed for a 6V/5A car headlamp bulb. To start with, the circuit in fig. 2 was used, the mains voltage of 220 V having in any case to be stepped down. The voltage being thus roughly stabilized, several transistors were connected in series with the lamp. These transistors are connected in such a way that they decrease the current as the amount of light incident on a photoresistor increases. The principle of the circuit is illustrated in *fig. 3*.

The stabilizing transformer *Tr* has two secondary windings, S_1 and S_2, of which S_1 serves for the lamp supply. The current of approx. 5 A is regulated by four type OC 16 transistors (T_2-T_5), connected in parallel in the common-emitter arrangement [3]). Since they pass the current in one direction only, they are bridged by a germanium diode D (type OA 31). The current through the lamp is therefore regulated only in one half of each cycle. An equalizing resistor of 1 Ω is connected in the emitter lead of each transistor in order to divide the current equally between them.

---

[1]) N. A. de Gier, W. van Gool and J. G. van Santen, Photoresistors made of compressed and sintered cadmium sulphide, Philips tech. Rev. **20**, 277-287, 1958/59 (No. 10).

[2]) H. A. W. Klinkhamer, A rectifier for small telephone exchanges, Philips tech. Rev. **6**, 39-45, 1941.

To explain how the regulation operates we shall first assume that the illumination is such that the bridge is balanced. If the illumination now increases, the value R_f of the photoresistor drops, causing the base of the amplifying transistor to go negative with respect to the emitter, and this transistor conducts. As a result the collector becomes less negative, and the same applies to the bases of the regulating transistors to which it is connected. From the transistor characteristics we may infer that this voltage increase cuts off the transistors as soon as the common collector voltage exceeds a certain value. Consequently, the current through the lamp is momentarily interrupted for a certain fraction of the active half of the cycle. The waveforms of the voltage across the incandescent lamp are represented in *fig. 5*.

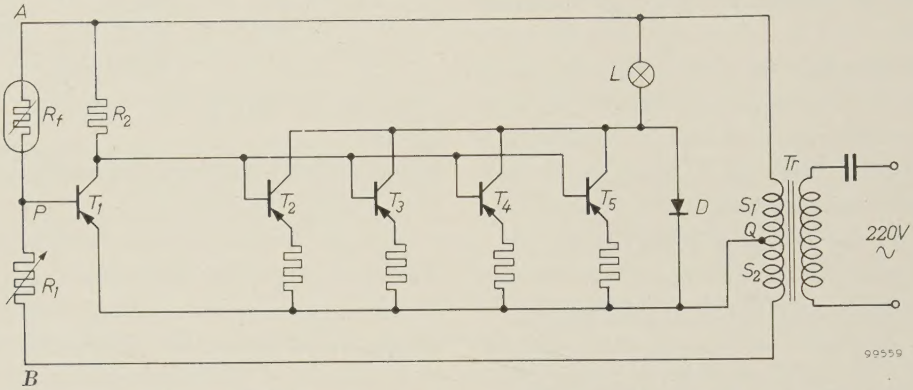

Fig. 3. Circuit for stabilizing luminous intensity. L incandescent lamp, R_f photoresistor, T_2-T_5 transistors regulating lamp current, T_1 transistor for amplifying control voltage.

Beside the lamp is mounted a cadmium-sulphide photoresistor (type ORP 30); it is enclosed in a can having a wedge-shaped aperture, which acts as a diaphragm for varying the illumination of the photoresistor (see *fig. 4*). This photoresistor (R_f in fig. 3) is included together with a variable resistor, R_1, in a bridge circuit, the other arm of which is formed by the secondary windings S_1 and S_2. Let the voltages in these windings be V_1 and V_2 and assume that they are in phase, then the bridge will be balanced (i.e. the voltage between P and Q will be zero) when $R_f : R_1 = V_1 : V_2$. This will be so only at one particular value of R_f, that is at a specific illumination of the photoresistor. A change in the illumination produces a voltage between P and Q. This voltage, the bridge output, is applied to the input of a transistor T_1, which acts as an amplifier and is again of type OC 16 in the common-emitter arrangement. The output voltage of T_1, developed across the resistor R_2, drives the four regulating transistors. The transistors are active only in that half of the A.C. cycle in which the collectors are negative; we need consider only this half cycle. (In the other half cycle the lamp is fed via the diode D.) In fig. 3, then, point A is negative with respect to point B.

In the inactive half cycle, the full current flows through the lamp via the diode. If the light source

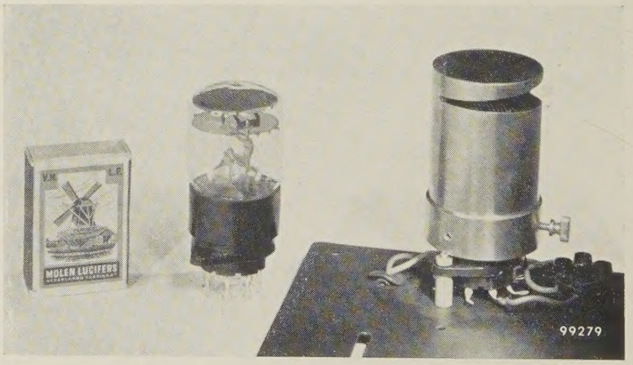

Fig. 4. Photoresistor, type ORP 30, mounted in a can with wedge-shaped aperture (diaphragm), seen from the light source. The light enters the aperture, where it is diffusely reflected so that every part of the horizontal photosensitive surface inside is equally illuminated. The illumination of the photoresistor can be varied by turning the can, which varies the effective width of the aperture. Left: the photoresistor shown separately.

---

[3]) J. P. Beijersbergen, M. Beun and J. te Winkel, The junction transistor as a network element at low frequencies, I, Philips tech. Rev. **19**, 15-27, 1957/58.

and photosensitive element were inertialess (as they would be if a discharge lamp and a high-vacuum photocell were used), the luminous intensity would accordingly not have the desired value during this half cycle. The regulation would then deal with only half the effect of a voltage variation. In fact, however, both the lamp and the photoresistor possess inertia. The luminous intensity does not follow the momentary change of the mains voltage, but remains at a value which is the average over several cycles. The regulation in the active half cycle is thus effective for voltage variations in the other half too.

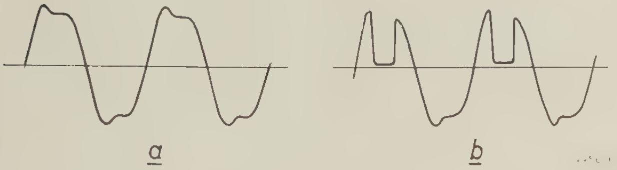

Fig. 5. Voltage waveform across the incandescent lamp, *a*) connected only to A.C. voltage stabilizer (which is responsible for the distortion of the sine wave), *b*) incorporated in the circuit described.

This control system does not lend itself well to a mathematical approach. The behaviour of the circuit can be very simply determined, however, by varying the magnitude of R_f in the absence of any feedback from the lamp to the photoresistor. For this purpose the photoresistor is replaced by a fixed resistance in series with a small variable resistance; the luminous intensity of the source is then measured as a function of R_f, at various voltages. What is in fact measured is not the luminous intensity I but the illumination E in a plane V perpendicular to the beam of light at the position of the photoresistor diaphragm (see *fig. 6*). Since luminous intensity and illumination are proportional to one another, we shall use E instead of I in the following considerations. The measured curves of $E = \varphi(R_f)$ are shown in *fig. 7*. It can be seen that a relatively slight decrease of R_f is indeed accompanied by a fairly considerable drop in illumination. The effect of the mains voltage in the absence of feedback is also apparent (the stabilizing action of the mains transformer is implicit in the curves).

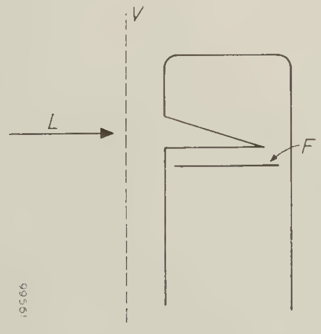

Fig. 6. Schematic cross-section of photoresistor with diaphragm. *F* photosensitive surface, *L* direction from which light enters diaphragm, *V* plane in which the illumination level is measured (*E* in fig. 7).

We can now represent the feedback graphically by plotting the line which indicates the value of R_f as a function of E. The characteristic of the photoresistor [4]) is such that R_f is inversely proportional to the illumination on the photosensitive surface. The value of this illumination is less than the above-mentioned E in the plane V, but the two values stand in a fixed relation to one another at any fixed position of the diaphragm. Hence R_f is also inversely proportional to E, and the relevant curve is part of a rectangular hyperbola $ER_f =$ constant. At a given setting of the diaphragm we obtain the line $R_f = f(E)$ represented in fig. 7. The operating point of the circuit at a particular mains voltage is now the point where this line $R_f = f(E)$ intersects the measured curve $E = \varphi(R_f)$. If the mains voltage changes, this point shifts along the line $R_f = f(E)$. Between 190 V and 250 V we see that E varies from about 79.5 to 80 lux, i.e. by about 0.5%.

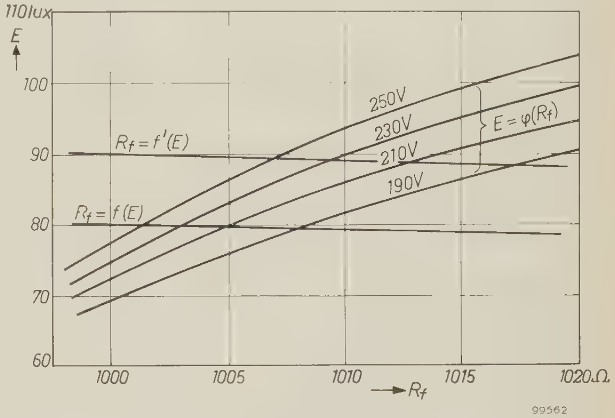

Fig. 7. Circuit characteristics, where E on the ordinate is the illumination at a fixed position just in front of the photoresistor diaphragm.

The curves $E = \varphi(R_f)$ are the characteristics of the circuit in the absence of feedback from lamp to photoresistor. The lines $R_f = f(E)$ and $R_f = f'(E)$ give the relation between E and R_f for the photoresistor, at two different positions of the diaphragm. At a given mains voltage the operating point of the circuit is the point of intersection between the relevant φ curve and f-line.

By changing the position of the diaphragm a different luminous-intensity setting is obtained. If we require a higher luminous intensity, for example, we turn the can (fig. 4) so that less light enters the diaphragm. Whilst E in plane V remains the same (fig. 6), the illumination on the photosensitive surface is now reduced. The resistance therefore increases, and the bridge is unbalanced. Point P in fig. 3 is now more positive, less current flows through T_1 and more current is passed by the regulating transistors. As a result, E increases, so that R_f again decreases until a new balance is reached. In this state of balance R_f will remain higher than before the change, inasmuch as more current must now flow through the lamp.

---

[4]) See fig. 7 in article [1]).

This can also be seen from fig. 7. If we consider only the line $R_f = f(E)$, distinct from the circuit, we see that it changes position when the diaphragm is reduced. Since R_f is larger for the same value of E, the line shifts to the right and is higher in the diagram than the original; see the curve $R_f = f'(E)$. The φ curves remain unchanged, so that the operating point at a given mains voltage now lies at a higher value of E. The value of R_f is also higher.

However, E now varies more than it did before with a given mains voltage fluctuation. Along the f-line the percentage change of E is equal to that of R_f (evidently, since differentiation of $ER_f =$ const. yields $dE/E = -dR_f/R_f$). The same applies to the f′-line. Upon a given change of R_f, then, $\Delta E/E$ is the same for both curves. An increase of E therefore means a proportional increase of ΔE, that is to say, a proportionally steeper slope of the line. Since the φ curves are roughly parallel with one another, it may be said that the variations referred to are proportional to E.

The circuit should be so adjusted as to allow the luminous intensity to be regulated for mains fluctuations in both directions. At 220 V, therefore, a part of each cycle should be suppressed, e.g. as shown in fig. 5*b*. For this purpose P in fig. 3 should be given a certain negative potential, which is done by varying R_1. Thus, in changing over to a different E setting, it is necessary to adjust both the diaphragm and R_1.

We shall now consider to what extent temperature variations affect the stability of the system. First, the effect on the photoresistor. The resistance of the CdS photoresistor increases by about 0.2% per °C temperature increase at 20 °C ⁵). This means that the f-line in fig. 7 is shifted 2 Ω to the right (0.2% of 1000 Ω). The φ curve corresponding to the nominal mains voltage remains unchanged; the operating point therefore moves to a higher position on this curve. If the φ curve were vertical, E would also increase by 0.2% (see above for f-line). Although the increase of E is somewhat smaller, the difference is negligible because the slope of the φ curves is much steeper than that of the f-lines. The increase in illumination when the temperature of the photoresistor rises by 1 °C can accordingly be put at 0.2%.

Temperature variations also affect the transistors; the most sensitive in this circuit is the amplifying transistor T_1. In an earlier article on transistors ⁶) it was shown that a temperature increase of 1 °C has the same effect as a voltage drop of 2.3 mV at the base (point P in our case). As a result the collector current rises, the collector goes more positive and the current through the lamp drops. This temperature effect is thus the opposite of that on the photoresistor.

The reduction of E can be calculated most simply by using the same reasoning as applied to the temperature effect on the photoresistor. The voltage drop at P, caused by the increased temperature of the transistor, can then be regarded as due to a drop in the value of the photoresistor. As in the preceding case, the φ curve then remains unchanged, but the f-line now shifts to the left. Here too, and for the same reason as above, the percentage change of E is roughly equal to that of R_f. We therefore have to find the decrease in R_f that causes a voltage drop of 2.3 mV at P. This follows directly from the formula for the output voltage V_0 of a Wheatstone bridge with identical resistances, one of which is varied:

$$V_0 = \tfrac{1}{4}\, V \frac{\Delta R}{R},$$

where V is the bridge supply voltage (15 V). For $V_0 = 2.3$m V we find a reduction $\Delta R/R$ of 0.06%, so that the decrease in E per °C increase in the transistor temperature may also be put at 0.06%.

It might be thought from the above that the two temperature effects would oppose each other, and that therefore the deviation should to some extent be compensated. In fact, the photoresistor and transistors do not undergo the same temperature variations, since they are in separate compartments in the actual apparatus. The most unfavourable case, i.e. oppositely changing temperatures, is very unlikely, however. Under the influence of the ambient temperature they are much more likely to change in the same direction. We are therefore on the safe side if we disregard the smaller of the two effects and reckon on a 0.2% increase per °C.

---

⁵) See fig. 8 in article ¹).

⁶) J. P. Beijersbergen, M. Beun and J. te Winkel, The junction transistor as a network element at low frequencies, III, Philips tech. Rev. **20**, 122-134, 1958/59 (No. 5).

Assuming temperature variations of 5 °C, this means light variations of 1%.

Because of these temperature effects the circuit is not constant enough to be used as a light standard, particularly since no account has been taken of phenomena associated with the aging of the photoresistor. However, for use with a colorimeter or spectrometer, where stability is required only during successive measurements on test and comparison samples, the influence of temperature is no objection.

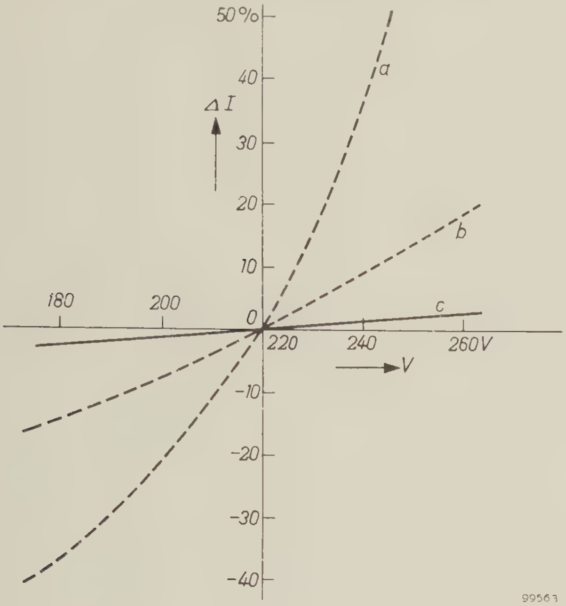

Fig. 8. Variation of the luminous intensity of an incandescent lamp with varying mains voltage. The curves show the percentage change of luminous intensity in relation to the value at 220 V, *a*) for lamp without stabilizer, *b*) for lamp fed by a simple voltage stabilizer as in fig. 2, *c*) for lamp incorporated in the circuit described. The curves *a* and *b* are those in fig. 1.

The photoresistor is mounted together with the lamp in one small compartment. Although this is ventilated, allowance must still be made for a warming-up period in which the luminous intensity increases. According to calculations the increase might be a few percent, and observation has also confirmed this. The luminous intensity has settled down to a constant value after about one hour, although the apparatus is stable enough for use after the first 20 minutes or so. A similar warming-up period is also prescribed for the spectrometer itself, for which the apparatus was primarily designed.

The apparatus is used at a luminous intensity twice as high as that at which the measurements for fig. 7 were done. On our reasoning this means that the variation of intensity with voltage should likewise be twice as high. The change, measured over a voltage excursion from 190 to 250 V, was in fact 1% (*fig. 8*).

Summary. A light source of constant intensity is commonly obtained by supplying an incandescent lamp from accumulators or a stabilized power supply. It is more logical, however, to stabilize the luminous intensity itself. A circuit designed for this purpose is described. The light source is a 6 V, 5 A incandescent lamp. The mains voltage of 220 V is first stepped down and stabilized by a transformer with a saturated core. A photoresistor in conjunction with five transistors regulates the luminous intensity. The latter remains constant to within 1% for mains voltage fluctuations of 20% in either direction. The effect of temperature variations is discussed; the intensity varies less than 0.2% per °C change in temperature.

FLYING-SPOT SCANNERS FOR COLOUR TELEVISION

by H. van GINKEL.

621.385.832:621.397.611.2

Flying-spot scanners for colour television are of interest chiefly because, in principle, their signals are completely free from errors of superposition or "register". The article below describes two types of flying-spot scanner that have rendered valuable service in development work on colour television at Philips. One is suitable for colour slides, the other for opaque objects (colour prints, drawings, small objects etc.). Both types probably have a useful part to play in colour television broadcasts.

Methods of generating primary colour signals

In colour television three camera tubes are used at the transmitting end, one for each of the three primary colours (red, green and blue) into which the incident light is split by special devices. The principles of such systems have been dealt with at some length in an earlier article in this journal ¹) which will henceforth be referred to as I. The three primary colour signals thus obtained are transmitted, as described in I, to the receiver. Here they are combined by a process of additive mixing to produce a multi-coloured picture, either on the fluorescent screen of a special direct-viewing tube, or on a projection screen on to which the three primary-colour images are projected ²).

In the development of the various circuits of a colour television system it is obviously necessary to have a signal source for the three primary-colour signals. These can be obtained from an electronic signal generator, a colour-television camera or a flying-spot scanner. The advantages and drawbacks of these three methods are mentioned below.

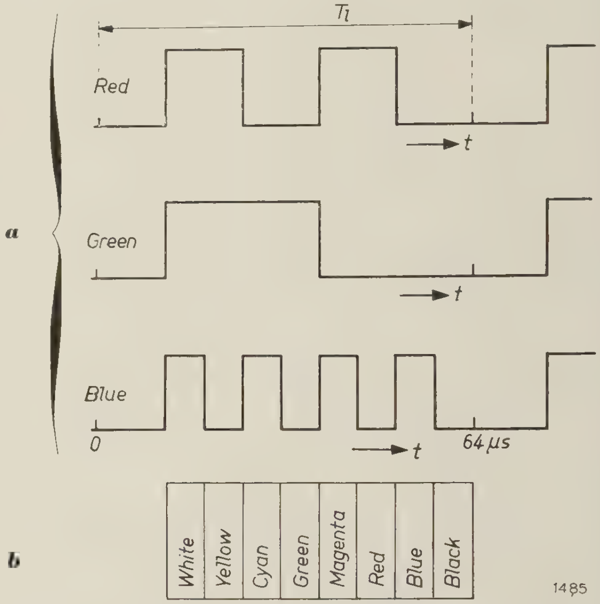

Fig. 1. *a*) Waveforms of primary-colour signals "red", "green" and "blue", produced by signal generators. T_l is the period of one complete line (scan plus flyback).
b) Combination of the three signals (*a*) produces a television picture consisting of vertical strips of the colours indicated.

a) *Electronic signal generator.* The signals represented in *fig. 1a* can be generated fairly simply. If they are used as "red", "green" and "blue" signals, respectively, a combination of them produces a television image consisting of variously coloured vertical strips (fig. 1*b*). This method, although it has the virtue of simplicity, is limited by its very primitive picture to only a few applications, such as testing certain properties of transmission systems.

b) *Studio camera(s).* The advantage of obtaining the primary-colour signals from studio cameras is that the situation is technically identical with an actual transmission and that the pictures can be given movement and detail. Apart from being more complicated, however, this method has the drawback that the signals delivered by a camera are subject, for reasons we shall explain, to slight errors. In experimental work this is a fundamental difficulty, for if the picture is unsatisfactory it is not usually known whether the cause lies in the part under investigation (transmission system, receiver, projector) or in the picture signals themselves.

Fig. 2 illustrates the path of rays in a camera containing three vidicons. As explained in article I (fig. 7) the light entering the camera is separated by dichroic mirrors ³) into three spectral components, red, green and blue, each of which is picked up by a separate vidicon.

---

¹) F. W. de Vrijer, Fundamentals of colour television, Philips tech. Rev. **19**, 86-97, 1957/58.

²) T. Poorter and F. W. de Vrijer, The projection of colour-television pictures, Philips tech. Rev. **19**, 338-355, 1957/58.

³) P. M. van Alphen, Applications of the interference of light in thin films, Philips tech. Rev. **19**, 59-67, 1957/58.

Because of light losses in the system, use is made only of highly sensitive camera tubes, such as image orthicons [4]) and vidicons [5]). The three primary-colour signals, one from each of the camera tubes, must be perfectly synchronized, i.e. the scanning beams in the three vidicons must pass corresponding image points at every instant. To meet this requirement it is essential to use identical objective lens systems and, by means of mirrors, to arrange the tubes in such a way that optically the three photoconductive layers apparently coincide. Further, the deflections — both horizontal and vertical — must have exactly the same amplitude, and even the unavoidable deviations from linearity (proportionality with time) should be equal. The latter is never entirely possible because there is always some spread in the properties of the components used; here, then, problems arise of the kind discussed in the article under [2]). The result of the failure to satisfy completely the conditions mentioned is that the three primary-colour images are out of register, i.e. they do not exactly coincide. Even if the reproduction system were faultless, the errors of register would still give rise to coloured edges between fields of different hue. The total picture then resembles a colour print on which the blocks were out of register during printing.

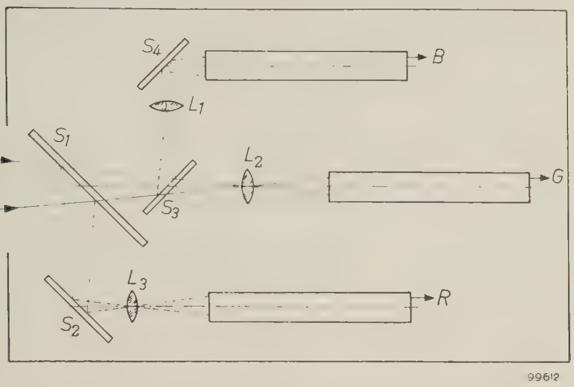

Fig. 2. Arrangement of the principal optical components and the vidicons in a colour-television camera, seen from above. *R*, *G*, *B* vidicons for red, green and blue, respectively. S_1, S_3 dichroic mirrors. S_2, S_4 ordinary mirrors. Light from the scene enters the system from the left. The red component is reflected by mirrors S_1 and S_2 and reaches the vidicon *R*; the blue component passes through S_1 and reaches the vidicon *B* via S_3 and S_4; the green component passes through both mirrors S_1 and S_3 and reaches vidicon *G*. The lenses L_1, L_2 and L_3 image the scene on the photoconductive layer of the vidicons. The images on the three vidicons and the individual scannings must be identical, otherwise some of the colour areas in the picture will show tinted edges.

c) Flying-spot scanner. A flying-spot scanner is used for generating a television signal from a flat object, such as photographic transparencies, prints, drawings, etc. An article on a flying-spot scanner for black-and-white slides appeared in this journal some years ago [6]). Its operation is recalled in *fig. 3*.

Fig. 4 shows how the flying-spot scanner can be extended to make it capable of generating three colour signals; the figure also incorporates a block diagram of the electronic equipment required. The dichroic mirrors are here in a cruciform arrangement (cf. [3]), fig. 12). The red, the green and the blue components are each picked up by a corresponding photomultiplier tube. Across the load resistor of each tube there thus appears a picture signal voltage, which is amplified and, as explained below, corrected for the afterglow of the phosphor and the non-linear relation between the luminous flux and the control voltage of the picture tube.

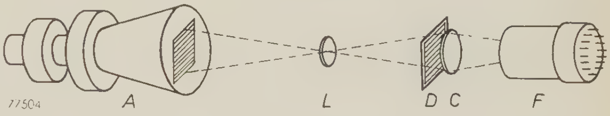

Fig. 3. Principle of a flying-spot scanner for black-and-white slides. The luminous spot on the cathode-ray tube *A* describes a line raster of constant brightness which is transmitted by the objective lens *L* on to the slide *D*. The condenser lens *C* collects the light transmitted by *D* and directs it on to the photocathode of the multiplier tube *F*. This luminous flux is proportional to the transmission of the transparency at each point scanned.

Since, in the system sketched, there is only one light spot on the cathode ray tube, and therefore only one light spot on the transparency, the three-primary-colour beams are perfectly synchronized. The same applies, then, to the three primary colour signals, and this is an important, fundamental advantage of the flying-spot scanner over the studio camera. Moreover, the flying-spot scanner is simpler in construction than a camera.

The principle of spot scanning need not be restricted in application to transparencies; it can equally be used for opaque matter such as prints and drawings.

In development work on colour television, wide use has been made of flying-spot scanners. They are indeed still employed at Philips for various purposes, as for example in factory inspection of direct-viewing tubes for colour television. In the following section we shall discuss a scanner for transparencies (colour slides), evolved in the Philips Research Laboratories [7]) and further developed by the ELA Division of Philips; in the last section a laboratory model of a scanner for opaque matter will be described.

---

[4]) See e.g. A. Rose, P. K. Weimer and H. B. Law, The image orthicon — a sensitive television pickup tube, Proc. I.R.E. **34**, 424-432, 1946.

[5]) P. K. Weimer, S. V. Forgue and R. R. Goodrich, The Vidicon photoconductive camera tube, R.C.A. Rev. **12**, 306-313, 1951. See also L. Heijne, P. Schagen and H. Bruining, An experimental photoconductive camera tube for television, Philips tech. Rev. **16**, 23-25, 1954/55, and L. Heijne, The lead oxide vidicon, Acta Electron. **2**, 124-131, 1957/58.

[6]) F. H. J. van der Poel and J. J. P. Valeton, The flying-spot scanner, Philips tech. Rev. **15**, 221-232, 1953/54.

Flying-spot scanner for colour slides

The scanning tube

The flying-spot scanner for black-and-white slides, described in article [6]), uses a cathode-ray scanning tube of the type that was discussed in the same issue [8]). The tube used for colour slides differs only in one respect — the spectral emission of the phosphor. In the former case it was simply a matter of generating radiation which would be transmitted with adequate contrast by the slide and to which the photomultiplier tubes were sensitive; apart from this the spectrum of the radiation is immaterial, unless of course colour slides are to be reproduced in a monochrome transmission. In colour television, however, the emitted light is required to possess all wavelengths of the visible spectrum; each point of the slide then transmits a certain proportion of some colours and thus absorbs a complementary proportion of the other colours.

Apart from the spectral distribution of the radiation, the luminous efficiency η and the afterglow time τ of the phosphor have to meet specific requirements. (η is the ratio of the radiant power emitted to the electrical power consumed, and τ is the time in which the emitted light decays to a fraction 1/e of its initial value after the sudden removal of the excitation.) The ratio $\sqrt{\eta}/\tau$ can be used as a figure of merit for the phosphor (see [6])) in the sense that, if its value is raised, the system comprising phosphor and photomultiplier will give a better signal-to-noise ratio. Among the phosphors used for colour television the best is found to be ZnO containing an excess of Zn. As can be seen from the spectral characteristic in *fig.* 5, this phosphor emits green light with a maximum at a wavelength of 505 mμ. Elsewhere the kind of ZnO phosphor used in colour TV is one where $\eta = 8\%$ and $\tau = 2.5$ μs. For our scanning tubes we prefer the kind having a luminous efficiency of 2.5% and an afterglow time of 1 μs. This is a somewhat longer afterglow than that of the gehlenite phosphor used for monochrome television. The consequences will be discussed presently.

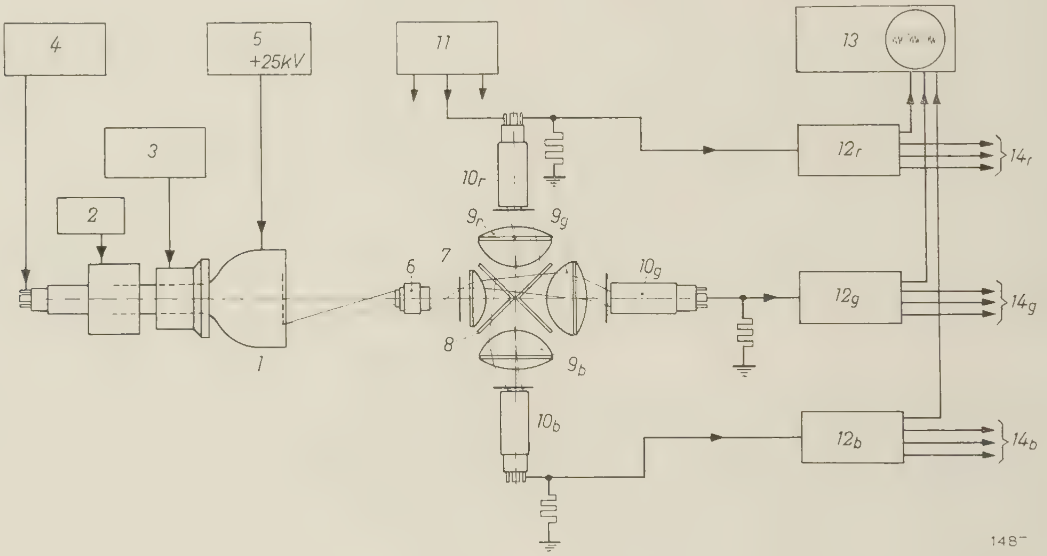

Fig. 4. Block diagram and optical system of a flying-spot scanner for colour slides. *1* scanning tube, *2* focusing coil, *3* generators for horizontal and vertical deflection, *4* stabilization of beam current and beam suppression during the flyback, and *5* anode-voltage generator (25 kV). *6* objective lens. *7* colour slide. *8* dichroic mirrors. *9* condenser lenses (the suffixes *r*, *g* and *b* relate to the "red", "green" and "blue" channels). *10* photomultiplier tubes (with filter in front of photocathode) and associated power pack *11*. *12* video channels with afterglow compensation, gamma correction and output amplifier. *13* test circuit with oscilloscope. *14* cables to black-and-white monitor, colour monitor and various signal consumer circuits.

---

[7]) The development work on this project was initiated by A. Wieberdink.

[8]) A. Bril, J. de Gier and H. A. Klasens, A cathode-ray tube for flying-spot scanning, Philips tech. Rev. **15**, 233-237, 1953/54.

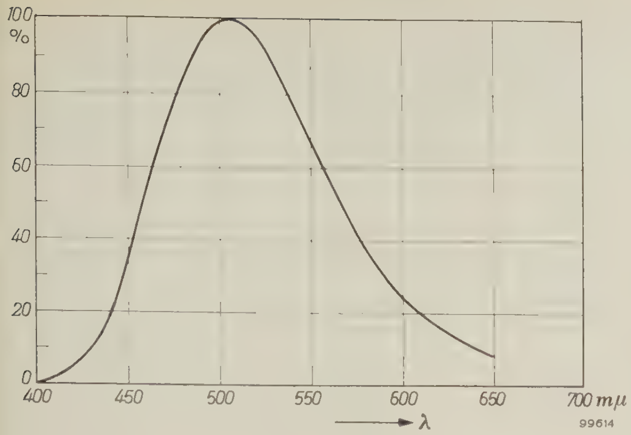

Fig. 5. Spectral characteristic of the light emitted by the ZnO-Zn phosphor employed in the scanner tube, measured in the Philips laboratories. Efficiency 2.5%. Afterglow time 1 μs.

Fig. 6 shows a scale drawing of the tube. The raster may be a maximum of 120 mm diagonally. The window is flat and must be entirely free of smudges and scratches, which would be imaged fairly sharply on the transparency. The electron gun is a triode type with an anode potential of 25 kV; as a rule the beam current is 150 μA. Magnetic focusing is employed.

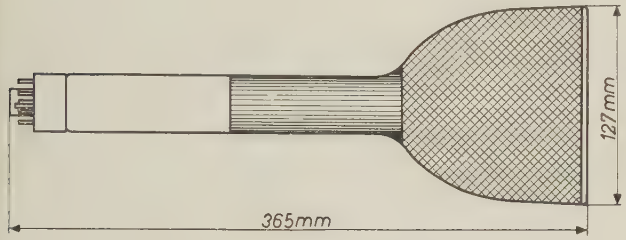

Fig. 6. Scale drawing of scanning tube.

The optical system

The path of the rays from tube window to photomultiplier cathode was illustrated in fig. 4. The major components of this optical system are the cruciform mirrors, the condenser lenses and the objective lens. To minimize light losses at the intersection of the mirrors (8 in fig. 4) the front mirrors, i.e. those facing the objective lens, are made thicker than the rear ones [9]).

The condenser lens system serves a dual purpose. Firstly, the condenser lens at the transparency side ensures that the beams emanating from points outside the middle of the raster are bent towards the axis of the system. This is done in such a way that the axes of these beams all reach the dichroic mirrors at virtually the same angle — in this case 45° — irrespective of their point of origin on the raster. This is necessary because the reflection coefficient of the mirrors is a function of wavelength, and hence the colour of the reflected light depends on the angle of incidence. Secondly, the condenser system serves to image the diaphragm of the objective lens on the photocathode (we shall return to this later). This is done by the lens at the transparency side in conjunction with the lens adjacent to the photocathode.

The objective lens is an anastigmat of aperture *f*. 2. When the flat raster on the tube, measuring 6×8 cm, was imaged with a reduction of 2.85 times on a colour slide measuring 21×28 mm, the definition at the edges proved to be perceptibly poorer than in the middle of the picture, even with smaller apertures. Improvement was effected by adding an auxiliary lens of +2.5 diopters.

Conversion of light into electric signal

As mentioned above, the light is converted into electric signals by means of photomultiplier tubes. The signal voltage delivered by these tubes (in our case 35 mV peak-to-peak) is high enough to discount the noise added by the amplifier.

One of the types of photomultiplier used in the flying-spot scanners is the Philips type 50 AVP photomultiplier tube [10]); a cut-away view of the tube appears in *fig.* 7. Each stage of this tube amplifies the current by a factor δ, the secondary emission coefficient. There are in all eleven stages, giving a total amplification of δ^{11}, which may be as high as 1 million times.

Because δ is raised to such a high power, the total amplification depends strongly on δ, and in its turn δ depends on the material of the dynodes and on the potential between successive dynodes. Fluctuations in these potentials therefore cause the amplification to vary. In monochrome television this gives rise only to variations of picture brightness. In colour television, however, there will in addition be colour variations if the amplification of the three photomultipliers varies unequally which, owing to unavoidable differences between individual tubes, is always the case. Variations in colour are much more troublesome than variations in brightness. The voltage of the source from which the dynodes receive their supply voltage must therefore be kept highly constant. Voltage-stabilizer tubes are used for this purpose.

---

[9]) See page 67 of the article under [3]). The idea is due to H. de Lang.

[10]) Also frequently used in scintillation counters; see Philips tech. Rev. **20**, 209-219, 1958/59 (No. 8).

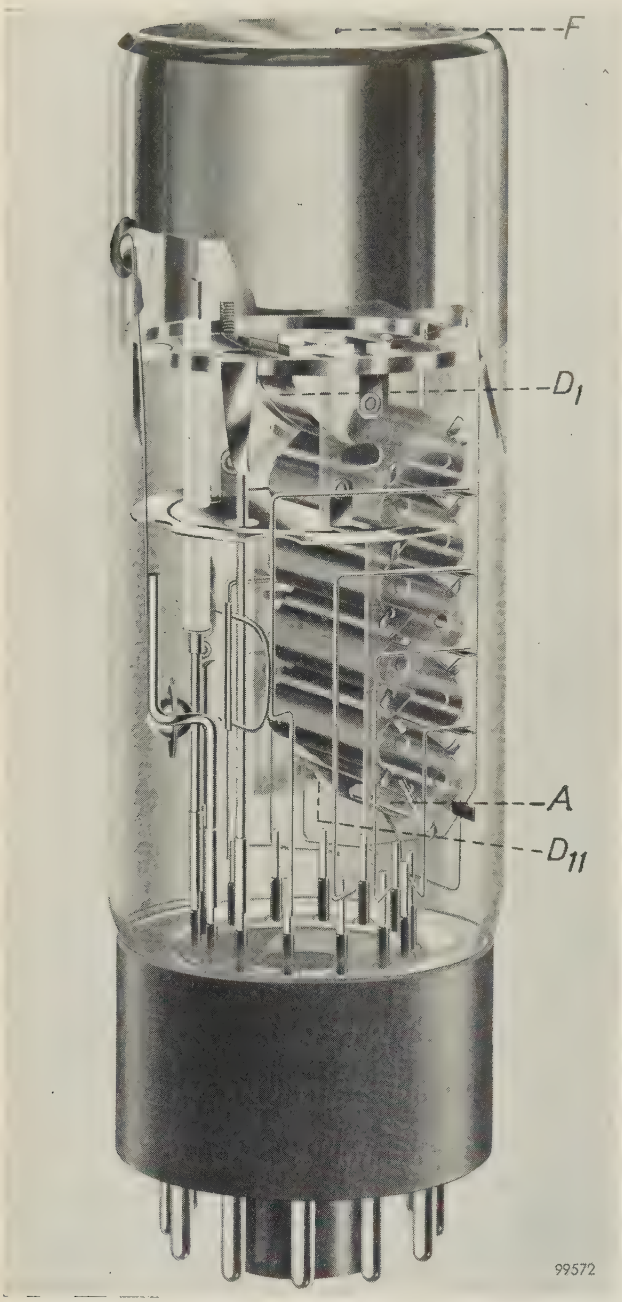

Fig. 7. Philips photomultiplier tube type 50 AVP. *F* photocathode. D_1 first dynode. D_{11} last dynode. *A* anode.

In general, the sensitivity of a multiplier tube is not uniform over the whole photocathode area. Furthermore, equal numbers of electrons issuing per second from various points of the photocathode will not always give rise to equal anode currents, owing to the fact that the first dynode is not an ideal collector. For these reasons, if the optical system were designed so as to image the slide itself on the photocathode, the resultant picture signal would show some slight modulation causing troublesome local colour differences to appear in the received picture. For this reason the diaphragm aperture, and not the slide, is imaged on the photocathode as mentioned earlier. The light originating from the luminous spot, and which has passed through the slide, is thus entirely "smeared out" over the part of the photocathode actually used.

The spectral sensitivity of the three channels

As remarked earlier, the scanning tube is required to emit radiation in the entire visible spectrum. This radiation, in so far as it is transmitted by the slide, is separated by the dichroic mirrors into red, green and blue components, which are picked up by the corresponding photomultiplier tubes. It was pointed out in article I that each of the channels thus formed must possess a very specific spectral sensitivity. The curves $\bar{R}(\lambda)$, $\bar{G}(\lambda)$ and $B(\lambda)$ in *fig. 8* can be interpreted as representing the anode currents of the respective photomultiplier tubes for light entering the optical system of continuously changing wavelength and of constant intensity. The parts of the curves below the λ-axis are usually disregarded for colour television (see I, page 92).

It is found that the use of dichroic mirrors as selective elements does not directly produce these curves, and for this reason a correction filter is introduced into the path of the rays, usually immediately in front of each photocathode. The spectral transmission $D_f(\lambda)$ of such a filter, e.g. $D_{fg}(\lambda)$ of the green filter, is calculated from the desired sensitivity $G(\lambda)$ and from the spectral energy distribution $F(\lambda)$ of the phosphor, the spectral

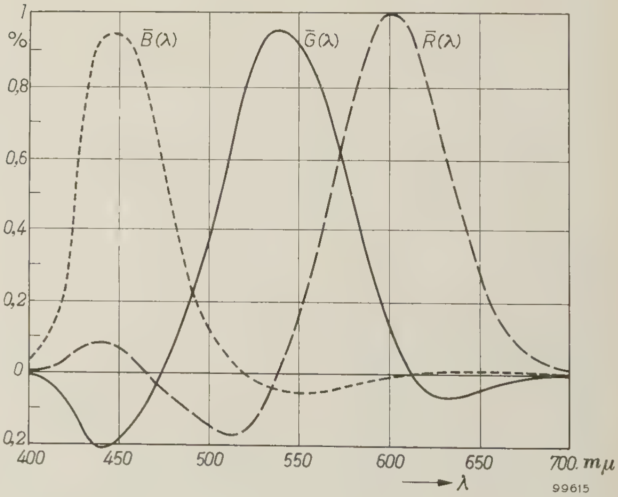

Fig. 8. Required spectral sensitivity of the three colour channels of a colour television system using primary colours whose colour points have the following coordinates:

red . . . $x = 0.67$, $y = 0.33$;
green . . . $x = 0.21$, $y = 0.71$;
blue . . . $x = 0.14$, $y = 0.08$.

Colourless objects are reproduced in standard white C, having the coordinates $x = 0.310$, $y = 0.316$.

transmissions $D_{\mathrm{r}}(\lambda)$ and $D_{\mathrm{b}}(\lambda)$ of the red and blue reflecting mirrors, and the spectral sensitivity $M_{\mathrm{g}}(\lambda)$ of the photomultiplier tube in the "green" channel:

$$D_{\mathrm{fg}} = \frac{\overline{G}(\lambda)}{F\,D_{\mathrm{r}}\,D_{\mathrm{b}}\,M_{\mathrm{g}}}\,.$$

All quantities in this expression are functions of λ. The desired transmissions D_{fb} and D_{fr} in the "blue" and "red" channels, respectively, are similarly found from:

$$D_{\mathrm{fb}} = \frac{\overline{B}(\lambda)}{F\,D_{\mathrm{r}}\,R_{\mathrm{b}}\,M_{\mathrm{b}}}$$

and

$$D_{\mathrm{fr}} = \frac{\overline{R}(\lambda)}{F\,D_{\mathrm{b}}\,R_{\mathrm{r}}\,M_{\mathrm{r}}}\,.$$

Here R_{b} is the spectral reflection of the blue-reflecting mirror and M_{b} the spectral sensitivity of the photomultiplier tube in the "blue" channel, whilst R_{r} and M_{r} are the corresponding quantities for the red-reflecting mirror and the photomultiplier tube in the "red" channel.

Fig. 9 shows the spectral characteristics of the cruciform arrangement of dichroic mirrors relating to each of the channels, i.e. $D_{\mathrm{b}}R_{\mathrm{r}}$ for the "red" channel, $D_{\mathrm{r}}D_{\mathrm{b}}$ for the "green" channel and $D_{\mathrm{r}}R_{\mathrm{b}}$ for the "blue" channel. In *fig. 10*, curve *1* represents the spectral sensitivity $F(\lambda)$ of the type 50 AVP photomultiplier tube. It can be seen from fig. 8 that the maximum of $\overline{B}(\lambda)$ lies in a region where the type 50 AVP multiplier still has 95% of its peak sensitivity. This tube is therefore used in the "blue" channel.

The maximum of $\overline{R}(\lambda)$ is found at $\lambda = 600$ mμ, and here the spectral sensitivity of the 50 AVP tube has dropped appreciably. From the spectral energy distribution of the phosphor used (see fig. 5) we find moreover that, compared with green, very little red light may be expected. Since the signal-to-noise ratio of the photocurrent is proportional to the root of the number of primary electrons per picture element, the "red" photocurrent will therefore have a poorer signal-to-noise ratio than the "green".

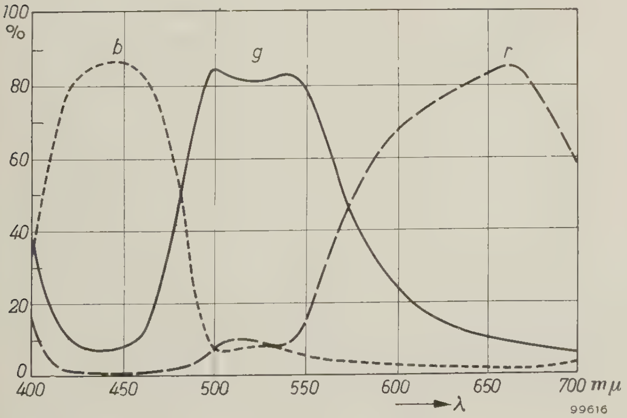

Fig. 9. Spectral characteristics of the cruciform arrangement of dichroic mirrors (*8* in fig. 4). As a function of wavelength λ the curve *r* represents the product $D_{\mathrm{b}}R_{\mathrm{r}}$, curve *g* the product $D_{\mathrm{r}}D_{\mathrm{b}}$ and curve *b* the product $D_{\mathrm{r}}R_{\mathrm{b}}$, where *D* denotes the transmissivity and *R* the reflectivity. The suffixes r and b represent red and blue, respectively. The curves relate to an angle of incidence of 45°.

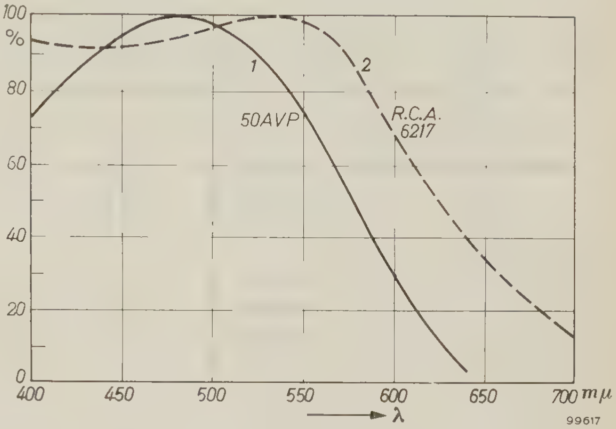

Fig. 10. Relative spectral sensitivity of two types of photomultiplier tube: Philips 50 AVP and R.C.A. 6217. Both curves are plotted relative to their peak sensitivity (= 100%). In the red region of the spectrum the type 6217 tube has a greater sensitivity, both relatively and absolutely.

This situation is worsened if, in order to bring the currents in the three channels to the same level, the 50 AVP tube is made to deliver a higher secondary-emission amplification by increasing the potential differences between the dynodes. Each multiplier tube adds to the signal current proper a noise component which is partly due to the presence of that current and partly to the "dark" current of the tube, which flows even when no light is incident on the photocathode. The dark current springs from several causes, such as thermionic emission from the photocathode, field emission from components of the tube, undesired photo-emission which occurs when fast electrons in the tube excite luminous phenomena that are "visible" to the photocathode, and finally leakage currents. Nearly all these unwanted effects become rapidly more serious if the voltage between the electrodes is raised in order to obtain a higher amplification. For this reason it was necessary in the case of the "red" channel to look around for a photomultiplier tube possessing a better spectral sensitivity in the red part of the spectrum than the type 50 AVP. The choice fell on the type 6217 tube made by the Radio Corporation of America; curve *2* in fig. 10 shows the spectral sensitivity of this tube (both curves are drawn with their peak sensitivity put at 100%).

The use of photomultiplier tubes specially sensitive to red has one disadvantage: the thermionic emission of the photocathode — which is part of the total dark current and has the character of noise — is troublesome even at room temperature. In spite of this, a 6217 tube is used in the "green" as well as in the "red" channel. The reason is that, if a 50 AVP were used, its decreasing sensitivity in the region from 540 to 610 mμ, in conjunction with the decreasing emission of the phosphor in the same region, would make a correction filter necessary having a relatively high absorption around the maximum of $G(\lambda)$; see fig. 8. If a more red-sensitive tube is taken, such as the type 6217, it is sufficient to use a fairly light yellow-transmitting filter. Since the phosphor emits its highest radiant power in the green part of the spectrum, the effect of noise is negligible.

Having decided on the types of photomultiplier tube to be used, we can calculate the spectral transmission characteristics of the necessary correction filters. The next step is to select from the filter manufacturers' catalogues the type of filter that best approaches the required transmission.

Fig. 11 shows the spectral sensitivities calculated for our slide scanners.

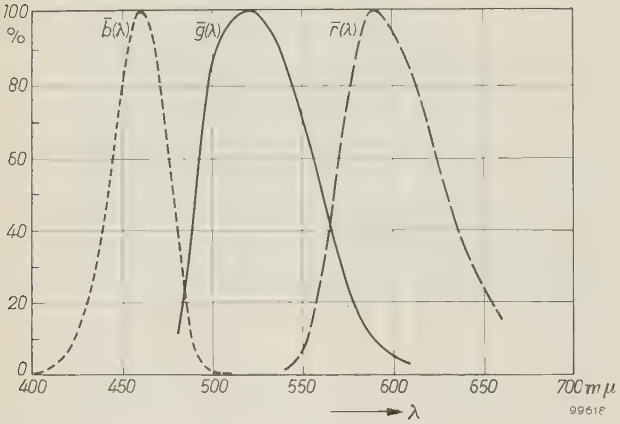

Fig. 11. Spectral sensitivity of the three colour channels (normalized to 100%) of the slide scanner, calculated from the known spectral characteristics of the phosphor, the dichroic mirrors, the correction filters and the photomultiplier tubes.

The electronic circuits

The deflection circuits and the extra-high tension generator of a flying-spot scanner for colour transparencies do not differ essentially from those published earlier. Since a flying-spot scanner is a signal source, higher demands are made on the linearity of the horizontal and vertical deflection than in picture tubes. The output voltage of the extra-high-tension generator is required to be extremely stable with respect to mains-voltage fluctuations, temperature variations and load variations. If the voltage is constant, the sharpness of the luminous spot on the cathode-ray tube need seldom be adjusted. This is particularly desirable in laboratory experiments, where different values of beam current may be used in fairly rapid succession. It may also be necessary now and then to vary the amplitude of the deflections; for this reason the extra high tension is taken from a separate generator and not, as is the practice in television receivers, derived from the horizontal deflection circuit.

The video amplifiers used in our flying-spot scanners for colour slides have a threefold function, viz.:

a) afterglow compensation,
b) gamma correction, and
c) distribution of the primary colour signals.

These functions are discussed in turn below.

a) *Afterglow compensation.* The phosphor on the screen of the scanning tube has the property of continuing to emit light for some time after excitation. Consequently the photomultiplier tubes receive light not only from the scanned picture element but also from picture elements previously scanned. Upon a sudden transition from dark to light or from light to dark in the slide, the picture signal therefore changes only gradually to the new value, resulting in a corresponding gradual transition in the received picture. This causes a certain unsharpness in the line scan of the picture, an effect also found if video amplifiers having too narrow a frequency band are used, i.e. the sharp transitions are blurred. Detailed quantitative considerations of afterglow are given in the article quoted under [6]). The circuit for afterglow compensation (*fig. 12*) is designed on the principles described in that article (p. 225). The basic idea is that the behaviour of the afterglow can be fairly accurately described by the sum of three exponential functions. In the cathode lead of the pentode in fig. 12 there are thus three *RC* networks whose time constants are made equal to those of the three exponential functions. One resistance and one capacitance are variable, in order to be able to make allowance for the aging of the phosphor.

Fig. 12 will be recognized as a circuit that selectively amplifies the higher frequencies (in that as the frequency rises the admittance of the capacitors bypassing the cathode resistors increases). This agrees with the described effect of the afterglow, namely that the system behaves like an amplifier with too narrow a frequency band; the band is widened by a circuit such as that in fig. 12.

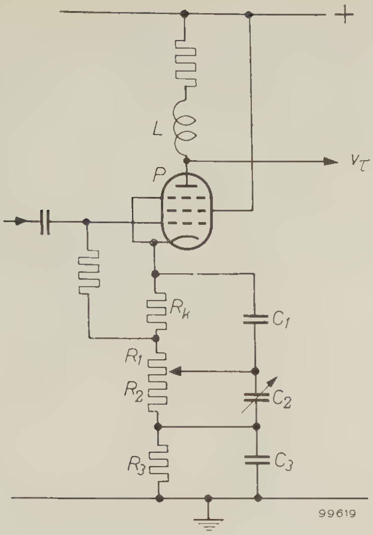

Fig. 12. Circuit for afterglow compensation. The sum of three exponential functions gives an approximation to the afterglow curve. The time constants $(R_k + R_1)C_1$, R_2C_2 and R_3C_3 of the *RC* networks in the cathode lead of the pentode *P* are made equal to the time constants of these three exponential functions. The magnitude of R_k ($\ll R_1$) determines the anode direct current. The ratio $R_1 : R_2$ is variable to allow for the properties of the phosphor changing with age. The inductance *L* in the anode circuit compensates for the loss in gain at high frequencies as a result of stray capacitances.

b) Gamma correction. The picture signal v_τ available following afterglow compensation is linearly proportional to the transmission of the slide. If this signal were directly used as a control signal for the picture tube, the picture produced would not give a true impression of the image on the slide. The reason is the non-linear relation between the luminous flux Φ and the control voltage V, which exists both in direct-viewing tubes and in projection tubes. As a rule the relation is $\Phi \propto V^\gamma$ (V measured from the cut-off point), where γ lies between 2.2 and 2.5. With suitable circuits, however, the signal v_τ can be made to produce a voltage $v \propto v_\tau^{1/\gamma}$, which is then suitable as the control signal, since $\Phi \propto v_\tau^{(1/\gamma)\gamma} = v_\tau$. In this way, then, we also linearize the last link in the transmission chain, namely the brightness of the picture tube.

The process by which a signal $v \propto v_\tau^{1/\gamma}$ is derived from the signal v_τ is called gamma correction. Many circuits have been devised for this purpose, and a feature common to all of them is that they contain one or more non-linear elements. The circuit used in our case is represented in *fig. 13a*. The triode *T* is arranged as a cathode follower. The variable resistance *R* is always large with respect to the resistance R_s, and R_s is large in relation to the resistance in the forward direction of the diode *D*. The resistance *R* is adjusted so that the D.C. potential of the point *e* is exactly equal to zero in the absence of a signal at *g*. *A* denotes a circuit functioning as a synchronous switch.

The synchronous-switch circuit *A* ensures that at point *g* the picture signal is zero during the flyback, i.e. when the scanning tube emits no light and the signal thus corresponds to black in the slide. The switch *A* is "closed" during the flyback or part of it; at times in between it is "open". (A circuit with a clamping diode can be imagined in place of *A*.)

As long as *A* is open the charge on the right plate of the coupling capacitor *C* cannot change; the potential of this plate thus varies together with that of the left plate, each scanning line, however, beginning from earth potential. We assume now that the input voltage v_τ has, say, a sawtooth waveform

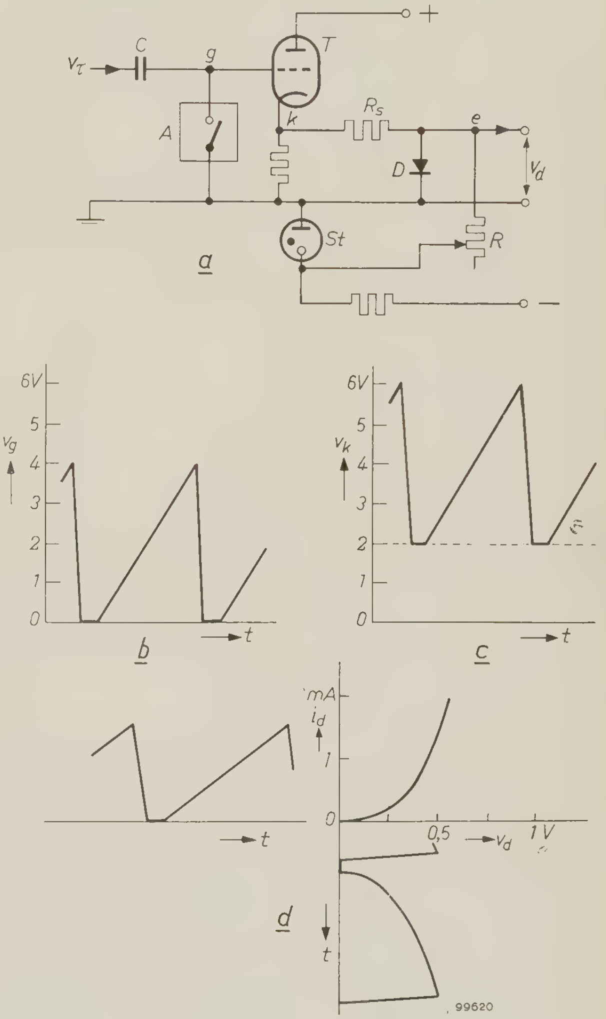

Fig. 13. *a*) Circuit for gamma correction. *T* triode, arranged as a cathode follower. *C* coupling capacitor. *A* is a circuit functioning as a synchronous switch, which suppresses the picture signal at point *g* during the flyback. *D* diode. *St* voltage reference tube. *R* resistor for reducing the D.C. potential at point *e* to zero, in the absence of a signal at *g*.
b) For the purposes of illustration it is assumed that the voltage v_g at point *g* in (*a*) has a sawtooth waveform.
c) The corresponding voltage v_k on the cathode.
d) A current i_d flows through the diode *D*. Owing to the curved characteristic of the diode, this current gives rise to an output voltage v_d having a curved sawtooth form, which compensates the opposite curvature of the characteristic $\Phi = f(V)$ of the picture tube.

(fig. 13*b*); through R_s and the diode the triode then sends a current i_d which is also of sawtooth shape (fig. 13*d*). Because of the curved characteristic of the diode the voltage v_d across the diode (likewise the output voltage) assumes a curved shape (fig. 13*d*). If we take a diode having a suitable characteristic we obtain $v_d \propto v_\tau^{0.4}$, which corresponds to $\gamma = 2.5$. For the three video amplifiers of a colour-slide scanner, three diodes are required that satisfy the above relation between 5 and 100% of the voltage range and in addition differ as little as possible in their individual characteristics.

The process described ensures that the dark parts are reproduced in the correct colour ratio, brighter than they would be without gamma correction. There are circumstances, however, in which an additional correction would be desirable, where some parts of the reproduced picture still appear too dark in relation to the bright parts. Such "hard" pictures may be obtained when contrasty slides are used. The contrast ratio of the slide, i.e. the ratio of the highest level of brightness to the lowest level of brightness, is then greater than that obtainable on the picture tube screen. The effect of this is that dark parts of the picture show too little contrast. With films and slides this is a frequent occurrence; since these are primarily intended for direct optical projection the difficulty does not arise here to the same extent, because an optical projector gives a higher contrast ratio than the picture tubes hitherto available for colour television. Sometimes it may be desirable for purely aesthetic reasons to reproduce dark parts with a relatively higher level of brightness.

The additional correction referred to can be obtained with a scanner for monochrome slides by reducing the exponent of the gamma correction (see article [6]) page 228). A glance at *fig. 14* shows that such a reduction is not permissible in the case of a scanner for colour slides. Suppose that we have selected $1/\gamma = 0.32$; then v_τ undergoes a correction $v_d' \propto v_d^{0.8}$ over and above the correction $v_d \propto v_\tau^{0.4}$. This can be seen in fig. 14. If a certain fragment of the image has a brightness level and a colour determined by the characteristic values *R*, *G* and *B* after the normal gamma correction, the additional correction would give this fragment a brightness and colour corresponding to the signals $R_{0.8}$, $G_{0.8}$ and $B_{0.8}$. This brightness level is indeed higher, as desired, but now the colour has changed too, since the "blue" signal has increased more than the "green" signal, and the latter more than the "red"; the colour balance has thus been destroyed.

The solution has been found in circuits that amplify the weaker picture signals more than the stronger ones, whilst preserving the existing ratio between the amplitudes of the "red", "green" and "blue" signals. A circuit meeting these requirements and used successfully in the Philips laboratories has been described elsewhere [11]).

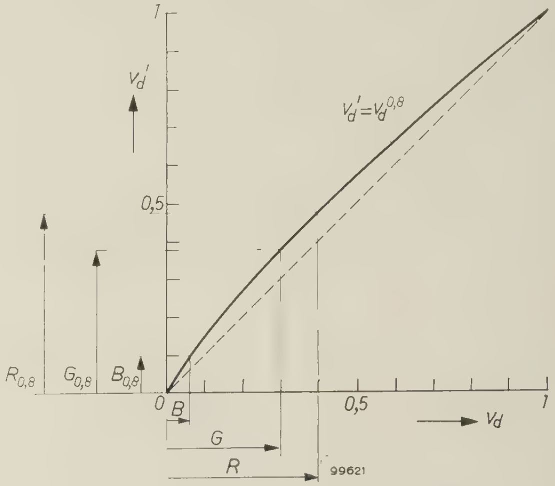

Fig. 14. If too hard colour pictures were corrected with the circuit in fig. 13*a*, they would not only become softer but also change colour, as illustrated here. *R*, *G* and *B* represent the three primary-colour signals (already gamma-corrected) which together constitute a patch in a colour picture which is desired to be softer. If each signal is passed through a circuit as in fig. 13*a*, having a characteristic $v_d' \propto v_d^{0.8}$, three additionally-corrected colour signals are obtained, $R_{0.8}$, $G_{0.8}$ and $B_{0.8}$, which are all greater in amplitude than *R*, *G* and *B* (a signal of value 1 would have remained unchanged). The relevant patch is thus made brighter. Whereas *R* and *G* have increased by 20 to 30%, *B* has almost doubled; the patch has thus changed in colour, which was not the intention.

c) Distribution of the primary-colour signals. The three colour signals have to be routed to a test circuit and various monitors, and also to the various destinations required for experimental purposes. In order to make the various load circuits independent of each other, an output stage having a very low internal impedance is necessary. This brings us to the third and last function of the video amplifiers, i.e. the routing of the corrected signals.

Fig. 15 shows the circuit diagram of the distribution stage used in each of the three channels. As mentioned in article I, the three primary colour signals are commonly standardized so as to give them equal amplitudes for white (where absorption in the slide is independent of the wavelength of the light). For the output voltage of the preceding stage we selected a peak-to-peak value of 1 V. This, then, is the input voltage of the distribution stage in fig. 15. After being amplified by the double triode T_1-T_2, the signal drives a pentode *P* arranged as a cathode follower. From the cathode of P negative feedback takes place via a resistor R_2 to the cathode of T_1. The voltage gain is just about equal to the ratio $(R_1 + R_2)/R_1$, where R_1 is the cathode resistance of T_1. Since $R_2 = R_1$, the potential at the point O is twice as high as the input voltage, i.e. 2 V peak-to-peak. Owing to the negative feedback the internal impedance is extremely low ($<$ 1 ohm).

---

[11]) J. Kaashoek, Gradationsentzerrung im Farbfernsehen, Nachr.techn. Z. **11**, 515-518, 1958.

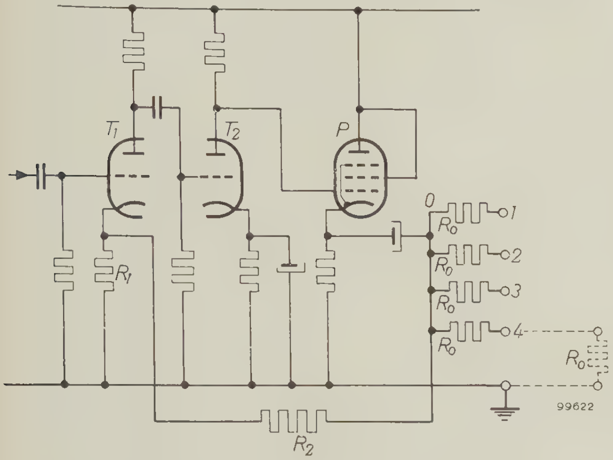

Fig. 15. Basic diagram of the distribution amplifier. T_1-T_2 double triode. P pentode as cathode follower. From the cathode of P feedback is effected via the resistance R_2 to the cathode of T_1 (with cathode resistance $R_1 = R_2$). *1, 2, 3, 4* are output terminals to which are connected cables (having a characteristic impedance R_0 and terminated by R_0), leading to a test circuit, monitors and the consumer circuits. Input voltage 1 V peak-to-peak. Voltage at O: 2 V peak-to-peak. Voltage at the end of the cables: 1 V peak-to-peak.

The four output terminals *1 . . . 4* are each connected to point O via resistors R_0. Connected to the terminals are cables, each of characteristic impedance $R_0 = 135$ ohms, which are terminated at the input end by the resistances R_0, and must be terminated at the other end by the same resistance. Across each terminating resistor there thus appears a signal of 1 V peak-to-peak. The four cables lead respectively to

1) a second distribution amplifier, to which the various consumer circuits are connected,
2) a black-and-white monitor, used for checking the definition and geometry of the picture and to help in fault-finding,
3) a colour monitor [12]), for critically appraising the colours, and
4) a test circuit for measuring the output signals.

The advantage of this method compared with the use of, say, a cathode follower in each of the four channels is that the signals on the terminals *1 . . . 4* are completely identical. If no anomalies are found on the monitors or with the test circuit, one can be quite sure that correct signals are being distributed. Owing to the low internal impedance, a disturbance at the end of one of the cables (e.g. due to a mismatch) is not noticeable at the other places.

Finally, a few words about the test circuit referred to. The three primary-colour signals are displayed simultaneously side by side on a cathode-ray oscilloscope. The oscilloscope is provided with a D.C. restorer, which ensures that the parts of the oscillogram corresponding to "black" are always at the same level. A transparent screen fitted over the oscilloscope screen is provided with a horizontal line, previously traced through the peaks of a sinusoidal calibrating signal [13]) of 1 V peak-to-peak and having the same frequency as the horizontal deflection. When a slide is changed, the waveform of the primary-colour signals is observed on the oscilloscope, and the diaphragm of the objective lens is adjusted until the peak of the largest of the three signals just reaches the line; this signal then has an amplitude of 1 V peak-to-peak.

When the scanner is first switched on, a black-and-white slide is first inserted and then, by varying the supply voltage, the amplification of the photomultiplier tubes is regulated until the three primary-colour signals have the same amplitude.

Figs. 16 and *17* show two flying-spot scanners for colour slides, built on the principle described. One is a laboratory version, the other a version further developed by the Philips ELA Division.

Flying-spot scanner for coloured prints

Single-reflection arrangement

Fig. 18a and *b* shows the simplest arrangement of a flying-spot scanner for opaque matter, for black-and-white only. The raster of the scanning tube *1* is projected as an enlarged image on to the print *3* which is to be reproduced. Depending on the density (blackening) at the place where the image of the luminous spot happens to be, a greater or lesser part of the incident light is reflected; the remainder is absorbed in the paper. Of the reflected light the photocathode of the multiplier tube *4* picks up the part bounded by the cone *5*; this part generates the output current, which causes the picture signal to appear across the signal resistor. The signal is passed through a video amplifier identical with that used in a slide scanner. Here too, of course, afterglow compensation

---

[12]) See, for example, fig. 19 in the article under [2]).

[13]) The calibrating signal is generated by an oscillator the principle of which is described in: L. Ensing and H. J. J. van Eyndhoven, An oscillator with constant output voltage, Philips tech. Rev. **14**, 304-312, 1952/53.

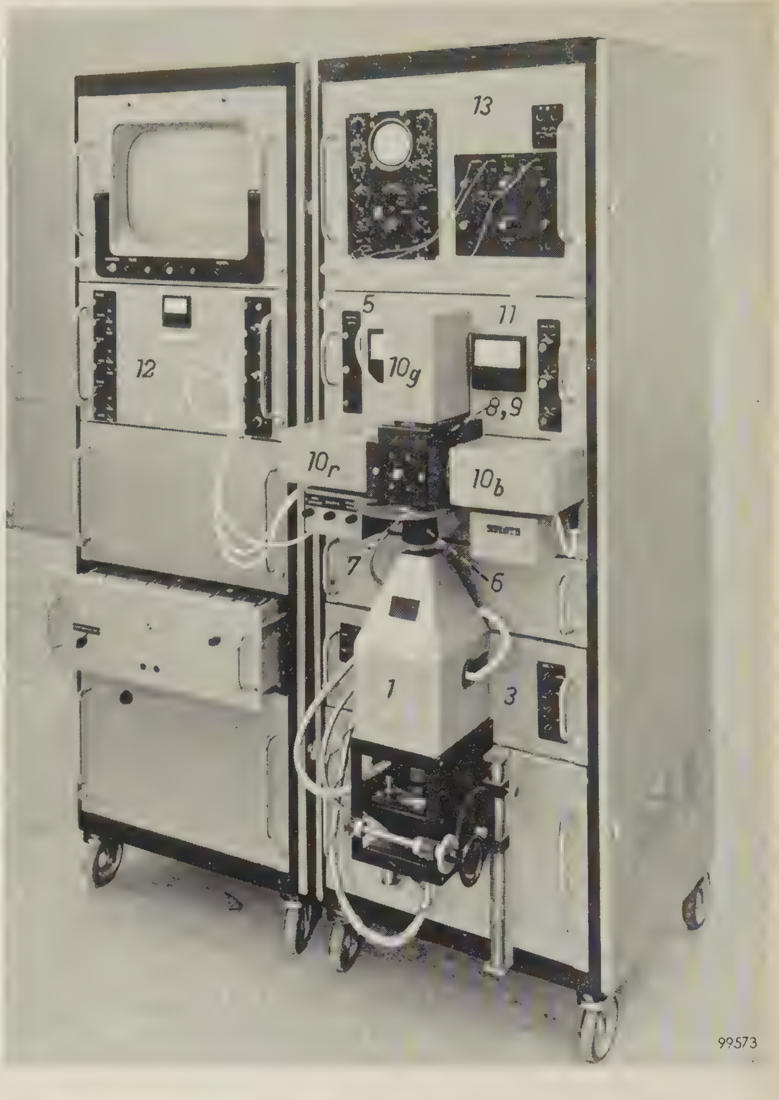

Fig. 16. Flying-spot scanner for colour slides, based on the principles described and built in the Philips Research Laboratories, Eindhoven. Meaning of figures as in fig. 4.

and gamma correction are equally necessary, to allow for the decay of the phosphor and the curved characteristic of the picture tube.

In the following we shall discuss some of the considerations underlying the design of a scanner for coloured prints.

If the print is a perfectly diffusing surface, the luminous intensity in any direction obeys Lambert's cosine law, irrespective of the direction from which the light strikes the surface. Let I_0 be the luminous intensity in the direction of the normal, then in a direction making an angle α with the normal the luminous intensity is $I_0 \cos \alpha$ (circular diagram, fig. 18*c*). If, on the other hand, the paper is glossy, the reflection is again diffuse except in directions near to the reflection angle equal to the angle of incidence. In these directions there is specular reflection, which is much stronger, and the diagram assumes the form of a lobe (fig. 18*d*), having a maximum and a width that depend on the nature of the glossy paper. Most photographs on art paper, as often used for colour reproductions, have reflecting surfaces of this kind, and so also have lacquered and plasticified types of paper as often used for advertisements and wrappings.

When the photomultiplier tube is positioned as shown in fig. 18*a*, the photocathode just remains clear of specularly reflected light (denoted by the dashed line). The luminous flux received by the photocathode from the middle and the edges of the

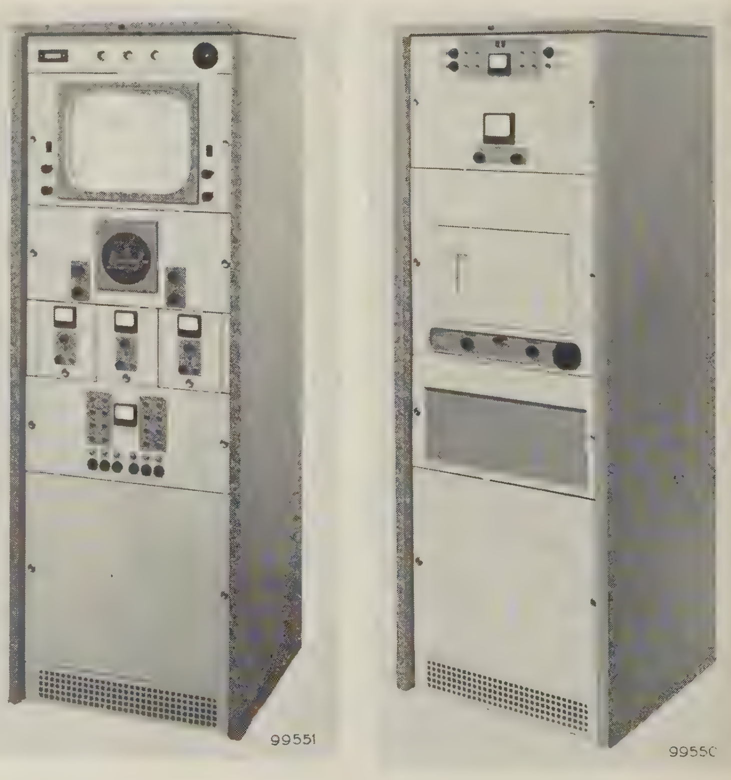

Fig. 17. The flying-spot scanner as in fig. 16, after further development under the direction of F. H. J. van der Poel in the ELA Division of Philips. The console on the left contains the monitor and the oscilloscope, that on the right the scanning tube, the optical system and the photomultiplier tubes.

paper, however, will differ. The angle δ can be so adjusted that most light will be received from the middle. The television picture will then show a vignetting effect to an extent that depends on the height of the multiplier tube above the paper and the distance from the optical axis. This effect, added to the unavoidable vignetting effect of the objective lens, may exceed the permissible limit if, in order to receive more light, the photomultiplier tube is positioned nearer to the print. In the case of colour television there is a further complication, in that three photomultiplier tubes have then to be arranged in such a way that the vignetting effect for all three is the same; otherwise, of course, colour defects would appear in the picture. All three photocathodes, then, should really have the same relative position. (This might be achieved by means of dichroic mirrors. These have not been used here, however, because of the light losses they cause and the constructional difficulties involved. In the arrangement such as in fig. 18*a* the light is separated into the three primary colours entirely by filters mounted in front of the photocathodes; we shall return to this point at the end of the article.)

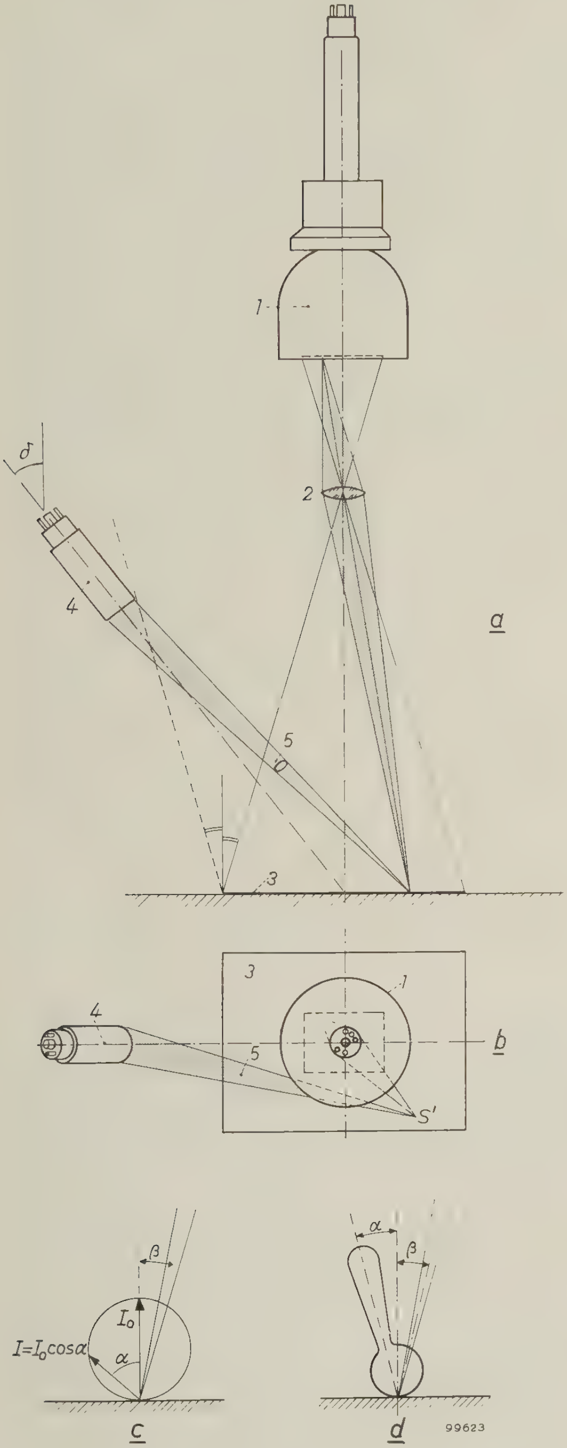

Fig. 18. *a*) Vertical section, *b*) horizontal projection, of a simple arrangement for a print scanner. *1* scanning tube. *2* objective lens which projects the raster on the scanning tube screen upon the print *3*. *4* photomultiplier tube. *5* cone within which the photocathode of *4* is seen by a scanned picture element *S* of the print.
c) Diffuse reflection: luminous intensity I in the direction α is proportional to cos α (Lambert's law), irrespective of the direction of incidence β.
d) Specular plus diffuse reflection from glossy paper: the luminous-intensity diagram shows a lobe in the direction $\alpha = -\beta$.

Another point of importance in a set-up as in fig. 18*a* is that careful precautions must be taken to prevent light other than that from the luminous spot from falling on to the print. "Alien" light in the first place produces an additional D.C. component in the output current; although the resultant direct-voltage component is easily removable from the actual picture signal, the additional current increases the noise, thus causing needless deterioration of the signal-to-noise ratio. The interfering light is usually artificial light from lamps operating on alternating current; this will therefore give rise to a second undesired effect in the picture signal, in the form of a hum component of twice the mains frequency. If the interfering light is relatively intense, it might in addition produce non-linear distortion phenomena.

The arrangement described below provides effective shielding against interfering light and considerably reduces vignetting effects.

Scanner using a photometer sphere

Fig. 19 illustrates a set-up in which the objective lens and the multiplier tubes are mounted in the wall of a hollow sphere provided with a diffusing white internal surface. The use of a photometer sphere offers an appreciable light gain [14]). The photo-

---

[14]) A print scanner using a photometer sphere for monochrome television is described in: H. Stier, P. Lindner and E. Kosche, Die Lichtpunktabtastung und die Übertragung episkopischer Bildvorlagen, Nachr.technik 5, 537-541, 1955.

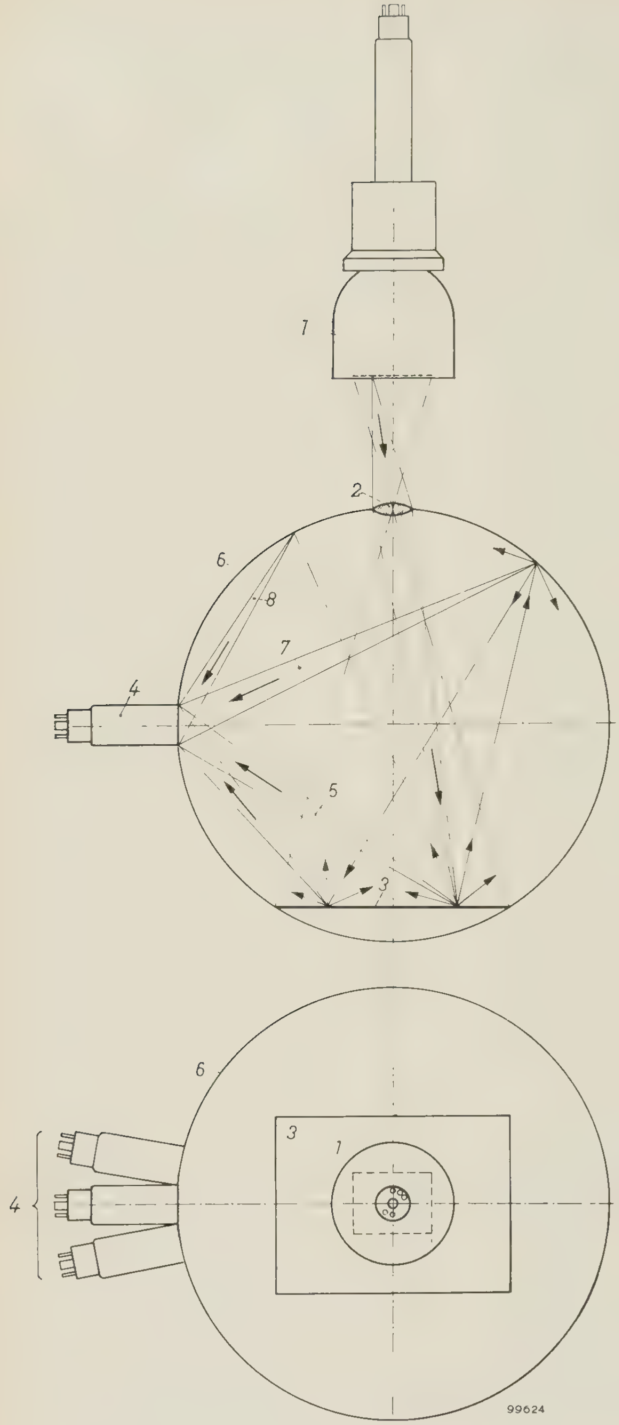

Fig. 19. Print scanner based on the use of a photometer sphere. *1* scanning tube. *2* objective lens. *3* print. *4* photomultiplier tubes. *5* cone of light directly incident on a photocathode. *7*, *8* cones of light reaching the photocathode after a single reflection from the wall of the photometer sphere *6*.

cathodes now receive not only the light reflected directly from the print (cone *5*) but also the light diffusely reflected once (cones *7* and *8*) or more than once from the wall of the sphere. The light that in fig. 18*a* was reflected outside the bounds of the cone *5* was entirely lost, whereas now a great deal of it reaches the cathodes. The gain provided by this integrating effect amounts to a factor F, given by the expression

$$F = \frac{1}{1 - A\varrho_{\mathrm{W}}},$$

where ϱ_{W} is the reflection coefficient of the white inner wall of the sphere, and A is the part of the wall participating in the diffuse reflection in relation to the total surface area of the sphere (the objective lens, the photocathodes and the print itself are considered to make no contribution to the diffuse reflection).

In *fig. 20a*, S represents a diffusely radiating surface. In a direction at an angle α with the normal to S the luminance L_α is by definition the ratio of the luminous intensity I_α (in candelas) and the effective surface $S \cos \alpha$ (in m^2), both seen from the direction α:

$$L_\alpha = \frac{I_\alpha}{S \cos \alpha} \text{ nit.}$$

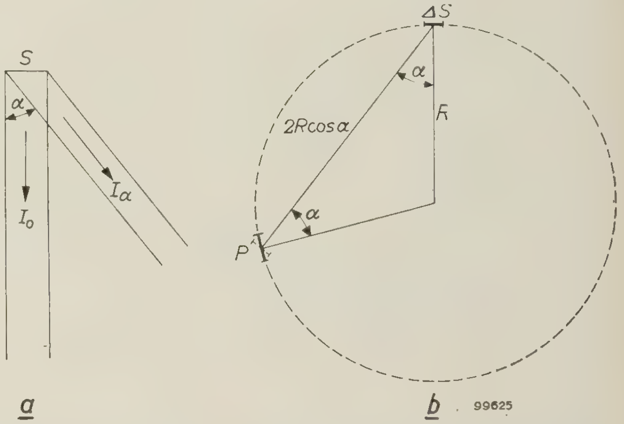

Fig. 20. *a*) In a direction α with respect to the normal, a diffusely radiating surface S that obeys Lambert's law has luminous intensity $I_\alpha = I_0 \cos \alpha$.
b) A surface ΔS, obeying Lambert's law, and a surface at P form part of an imaginary sphere of radius R. It is shown in the text that the illumination of the surface at P is independent of the location of P on the sphere.

If the luminance is the same in all directions, it follows that

$$I_\alpha = L\, S \cos \alpha = I_0 \cos \alpha,$$

where $LS = I_0$. $I_\alpha = I_0 \cos \alpha$ is simply Lambert's law. The luminous flux Φ emitted by the surface S, where Lambert's law is obeyed, is calculated to be:

$$\Phi = \pi I_0 \text{ lumens.}$$

In fig. 20*b* the surface ΔS represents a diffuse light source of this kind, having a luminance L. The luminous intensity in the direction α is then $L\Delta S \cos \alpha$. We now calculate the illumination E_p on a surface through the point P, which surface, like ΔS, forms part of an imaginary sphere of radius R. For E_p we can write:

$$E_p = \frac{L\Delta S \cos \alpha}{(2R \cos \alpha)^2} \cos \alpha = \frac{L\Delta S}{4R^2}.$$

The illumination is thus independent of the place where P is situated on the wall of the (imaginary) sphere.

For the emitted luminous flux Φ we can write $\Phi = \pi I_0 = \pi L \Delta S$, and therefore $E_p = \Phi/4\pi R^2$.

In the arrangement shown in fig. 19 let Φ be the luminous flux entering the photometer sphere through the objective lens, and let ϱ_p be the reflection coefficient of the paper at the position of the luminous spot at a given moment. Then $\varrho_p \Phi$ is the luminous flux reflected by the print at that moment. Assuming that the print obeys Lambert's law, the wall of the sphere receives a uniform illumination of intensity $E_1 = \varrho_p \Phi/4\pi R^2$ (disregarding for the present the reflections from the sphere wall). Certain parts of the sphere wall, however, are not painted white, namely the objective lens, the photocathodes and the print itself. We assume that these parts do not reflect at all, and take this into account by the factor A $(< 1) =$ white surface area/total sphere surface area. If ϱ_w be the reflection coefficient of the white part, and $\varrho_p \Phi$ the luminous flux emanating from the print, the luminous flux reflected by the wall for the first time is $A \varrho_w \varrho_p \Phi$. This returns into the sphere and increases the illumination by an amount $\Delta E = A \varrho_w \varrho_p \Phi / 4\pi R^2$. This process is repeated an infinite number of times. The total illumination finally becomes:

$$E = \lim_{n=\infty} \frac{\varrho_p \Phi}{4\pi R^2} (1 + A\varrho_w + A^2 \varrho_w^2 + \ldots + A^n \varrho_w^n) =$$

$$= \frac{\varrho_p \Phi}{4\pi R^2} \frac{1}{1 - A\varrho_w} . \quad \ldots \ldots \quad (1)$$

Without the photometer sphere the illumination would be:

$$E_1 = \frac{\varrho_p \Phi}{4\pi R^2} . \quad \ldots \ldots \ldots \quad (2)$$

By using the photometer sphere we thus gain a factor

$$F = \frac{1}{1 - A\varrho_w} \quad \ldots \ldots \ldots \quad (3)$$

in the illumination of the sphere wall, and hence in the luminous flux incident on the photocathodes.

In *fig. 21* the gain factor F is plotted as a function of ϱ_w, for various values of A. It may be noted at this stage that the sphere can be given a reflection coefficient ϱ_w of 0.95 (we shall return to this later). It can be seen from fig. 21 that with A = 0.85, 0.90 and 0.95 (i.e. with respectively 15, 10 and 5% of the sphere wall non-reflecting) the gain factor is respectively about 5, 7 and 10. The choice of A will also be dealt with later.

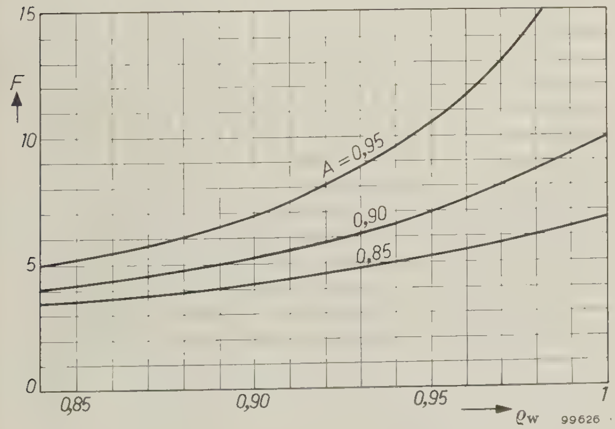

Fig. 21. The gain $F = (1 - A\varrho_w)^{-1}$ in luminous flux on the photocathode when using a photometer sphere, as a function of ϱ_w for various values of A.

Apart from the appreciable gain in light, important advantages of the sphere are that it shields the system against interfering light and greatly reduces the vignetting effects mentioned above. A further advantage is that the sphere attenuates the colour defects caused if the scanner is used for displaying small three-diemensional objects. In a scanner without such a sphere the objects are seen by the photomultiplier tubes from slightly different directions, with the result that they appear in the picture with coloured edges. The sphere largely eliminates this effect.

Comparison of luminous fluxes on the photocathodes in scanners for slides and for prints

In order to compare the luminous flux on the photocathodes in scanners for slides with that on the photocathodes in print scanners we first calculate, with the aid of *fig. 22*, the luminous flux Φ' which, at a given luminance L of the spot, is emitted from the objective lens. We assume that the phosphor obeys Lambert's law, i.e. that the luminous intensity of the spot at an angle α with the normal is $I_0 \cos \alpha$; the solid angle ω subtended at the objective by the spot is assumed to be so small, however, that we may put $\cos \alpha = 1$. Within the solid angle ω the luminous flux radiated is then $\Phi = \omega I_0 = \omega L \Delta s$, where Δs is the surface area of the spot. Let the transmission of the objective be τ_0; the luminous flux Φ' radiating from the objective is then

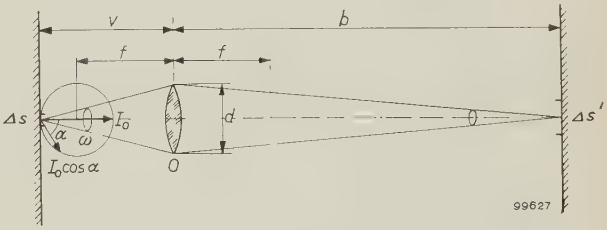

Fig. 22. Image formed of the luminous spot (surface area Δs) on the object to be reproduced (slide or print) by means of an objective lens O of diameter d and focal length f. The object distance is v, the image distance b.

$$\Phi' = \tau_0 \omega L \Delta s . \quad \ldots \ldots \quad (4)$$

To simplify the comparison we use the relations $\omega = \frac{1}{4}\pi d^2/v^2$, $d = f/c$ and $v = fN/(1 + N)$ to reduce equation (4) to

$$\Phi' = \frac{\pi \tau_0 L \Delta s}{4c^2} \left(\frac{N}{1 + N}\right)^2 , \quad \ldots \ldots \quad (5)$$

where $c = f/d$ is the aperture of the objective, i.e. the ratio of its focal length to its diameter, and N is the magnification $= |b/v|$ (b = image distance, v = object distance; see fig. 22).

a) Slide scanner. The luminous flux Φ' falls on the colour slide and the light passes successively (fig. 4) through the slide, the first condenser lens, the dichroic mirrors, the second condenser lens and the correction filter. The luminous flux Φ_s' finally incident on the photocathodes is

$$\Phi_s' = \tau_s \, \tau_{os} \, \tau_{ms} \, \tau_{fs} \times \tfrac{1}{4}\pi L \Delta s \left(\frac{N_s}{1 + N_s}\right)^2 \times \frac{1}{c_s^2}, \qquad (6)$$

where

τ_s is the spectral transmission of the colour slide,

τ_{os} is the transmission of the objective lens,

τ_{ms} is the spectral transmission of the dichroic mirrors and the condenser lenses together, and

τ_{fs} is the spectral transmission of the correction filter.

(The suffix s denotes the case of the slides.)

b) Print scanner (with photometer sphere). Here the luminous flux Φ' is reflected from the print, and the photocathodes pick up the reflected light, in part directly and in part after single or multiple reflections from the wall of the sphere. The luminous flux incident on the photocathodes is equal to the illumination E of the sphere wall times the effective surface of the photocathode (of radius r) times the spectral transmission of the filter. Introducing the suffix p to denote the case of the print scanner, we thus have $\Phi_p' = E \times \pi r^2 \times \tau_{fp}$, from which, in conjunction with (1) and (3), we obtain:

$$\Phi_p' = \varrho_p \tau_{op} \tau_{fp} \frac{r^2}{4R^2} F \times \tfrac{1}{4}\pi L \Delta s \left(\frac{N_p}{1 + N_p}\right)^2 \times \frac{1}{c_p^2}. \qquad (7)$$

In order to compare Φ_s' and Φ_p', i.e. (6) and (7), we make the following assumptions:

1) The raster on the scanning tube is the same size in both cases and the same beam current is used, so that $\frac{1}{4}\pi L \Delta s$ is equal in both cases.
2) $\tau_{os} = \tau_{op}$ (the objective lenses have the same transmission).
3) $\tau_s = \varrho_p$ (the spectral transmission of the transparency is equal to the spectral reflection coefficient of the print).
4) $\tau_{ms} \times \tau_{fs} = \frac{1}{2}\tau_{fp}$ (mirrors and filters of the slide scanner together have the same spectral transmission as the filter in the print scanner, and the transmission of glass bodies, such as the condenser lenses and the bases of the dichroic layers, is assumed to be 0.5).

With these assumptions we find from (6) and (7):

$$\frac{\Phi_s'}{\Phi_p'} = \frac{2}{F}\left(\frac{R}{r}\,\frac{c_p}{c_s}\,\frac{N_s}{1 + N_s}\,\frac{1 + N_p}{N_p}\right)^2 . \; . \; . \qquad (8)$$

For the slide scanner described we have: $N_s = 0.367$ and $c_s = 2.8$ (this lens aperture is the one most commonly used). For the print scanner, described below, we have: $F = 6.9$ (obtained from $A = 0.90$ and $\varrho_w = 0.95$), $N_p = 3$, $c_p = 2.5$, $R = 20.2$ cm and $r = 2.3$ cm (in the case of the R.C.A. tube type 6217). These values inserted in (8) yield: $\Phi_s' = 2.3\ \Phi_p'$. If the assumptions made are valid, the photocathodes in the print scanner receive a luminous flux which is 2.3× less than that in the case of the slide scanner. In order to obtain voltages of the same amplitude at the output of the video amplifiers it is therefore necessary to increase the amplification of the photomultiplier tubes by a factor of 2.3, which will give rise to a slight decrease in the signal-to-noise ratio.

Of course, one might also try to modify the above assumptions in such a way as to improve the calculated ratio of Φ_s' to Φ_p', possibly even to make Φ_p' larger than Φ_s'. This brings us to the question of the design and dimensioning of the print scanner.

Design and dimensioning of the print scanner

The first point of importance is the size of the prints to be reproduced. It was decided that the maximum size of print to be scanned should correspond to the printed part of a quarto format, i.e. 18×24 cm. Since the raster on the scanning tube is usually 6×8 cm, the magnification has to be $N_p = 3$.

Another design parameter is the radius R of the sphere, and in deciding on this it is necessary to take the factor A into account. It is desirable that A should be as close as possible to 1, in the first place because, according to (3), the gain factor obtained from the sphere is then greatest. Another reason is that, if A is small, there is a risk of colour poisoning. In defining A we assumed that the prints (and also the objective lens and the photocathodes) had no part at all in the reflections. In reality, of course, there are reflections from the print, and their influence on the colour rendering is evident if we consider the extreme case of a print which is entirely red except for a small green patch. The "green" signal produced when this patch is scanned will be weaker than it would be if the rest of the print were also green. The effect diminishes the smaller is the surface area of the print in relation to that of the sphere, that is the higher the value of A. Since the joint surface area of objective lens, photocathode and print is more or less fixed, A can only be raised by increasing the radius R. It appears from (8), however, that the ratio of the luminous fluxes $\Phi_p' : \Phi_s'$ is proportional to R^2, so that increasing R would be greatly to the disadvantage of the print scanner compared with the slide scanner as regards the luminous flux on the photocathodes. By way of compromise we decided on $A = 0.9$, which, with the given dimensions of print and photocathodes (those of the objective lens can only be estimated) leads to $R = 20$ cm.

If the objective is fitted in the sphere wall (fig. 19) the focal length f, now that R and the magnification N_p are fixed, is also determined and is, in this case, 9.25 cm. Lenses of this focal length and of f-number $c = 2.5$ are commercially available.

Finally, a few words about the way in which the inside of the sphere can be made reflective. From the optical point of view a vapour-deposited coating of magnesium oxide approaches the ideal, in that it obeys Lambert's law and has a reflection coefficient of 0.98. Its adhesion, however, leaves much to be desired. The article quoted under 14) refers to a mixture of ground MgO with a solution of gelatin in sufficient water to produce a spray-paint; the reflection coefficient mentioned is 0.95. Experiments at Philips have resulted in a similar paint, but using lithopone (a mixture of ZnS and $BaSO_4$) instead of MgO; this showed somewhat better adhesion and its reflection coefficient is 0.955. With $A = 0.9$ the gain factor F is 7 (fig. 21). (For photometric purposes it is more important to have a durable paint than to achieve the utmost in light economy; the paint commonly used in integrating photometers has a reflection coefficient of 0.90, which would give an F of only 5.)

Some constructional details of the print scanner

On the lines described above an experimental print-scanner has been designed, the optical components of which appear in *fig. 23.* A cross-section of the scanner is shown in *fig. 24.* The first thing one notices is that the sphere has been replaced by a cube with cut-off corners. This is assembled from a frame fitted with rectangular and triangular cover plates, which are readily removable if a fresh coating of paint is necessary. The three photomultiplier tubes are mounted in a triangular arrangement in a box which, for the purposes of experiment, can be secured at different places. As indicated by a dashed line, none of the photocathodes can receive any light reflected specularly from flat glossy prints.

The second point to be noted is that the scanning tube is positioned horizontally. The vertical position shown in fig. 19, with the screen pointing downwards, is undesirable because of the danger of damage being caused to the phosphor layer by loose particles in the tube. A plane mirror at an angle of 45° reflects the light downwards, enabling the print to be placed in a horizontal position.

It can further be seen that the objective lens is not mounted in the wall of the cube but between the scanning tube and the mirror (the focal length must accordingly be greater than mentioned above). Both the tube and the objective lens can be slid along the frame on which they are mounted, thereby making it possible to "enlarge" parts of 18×24 cm prints or smaller prints. Fig. 24*a* shows the situation for scanning a print of 18×24 cm, fig. 24*b* the case for a print of only 11×14.5 cm. This "optical enlargement" can be supplemented by "electrical enlargement", that is to say by reducing the size of the raster on the tube window. If this is done over a long period, however, there is a risk of a burn mark appearing on the phosphor, which will be visible in the picture when reverting to a raster of normal dimensions.

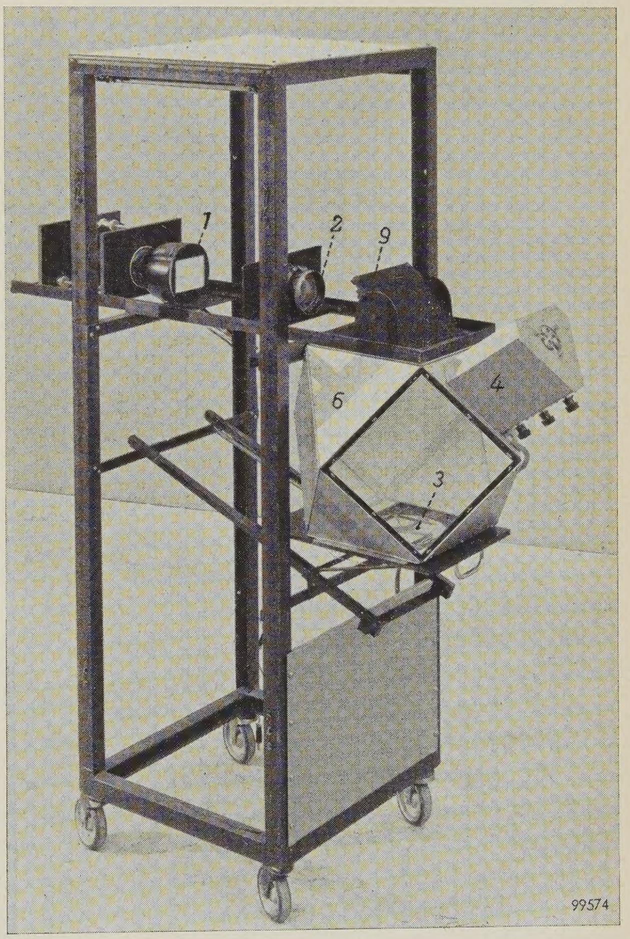

Fig. 23. Experimental print-scanner for colour television, built in Philips Research Laboratories, Eindhoven, photographed in the absence of the electrical sub-units to make the optical system clearer. *1* scanning tube. *2* objective lens. *3* print (here a test plate). *4* housing containing the three photomultiplier tubes. *6* "photometer sphere", here a cube with cut-off corners (one side plate has been removed to show the interior). *9* plane mirror at an angle of 45°.

As may be inferred from formula (7), enlargement will have the effect of decreasing the luminous flux on the photocathodes, and hence the output signal: in "optical enlargement" the magnification N_p of the optical system is actually *reduced*, and in electrical enlargement Δs is reduced. The loss of light can be considerably diminished, however, by covering the non-reproduced part of the print with a white surround; this then increases A, and moreover lessens the risk of colour poisoning.

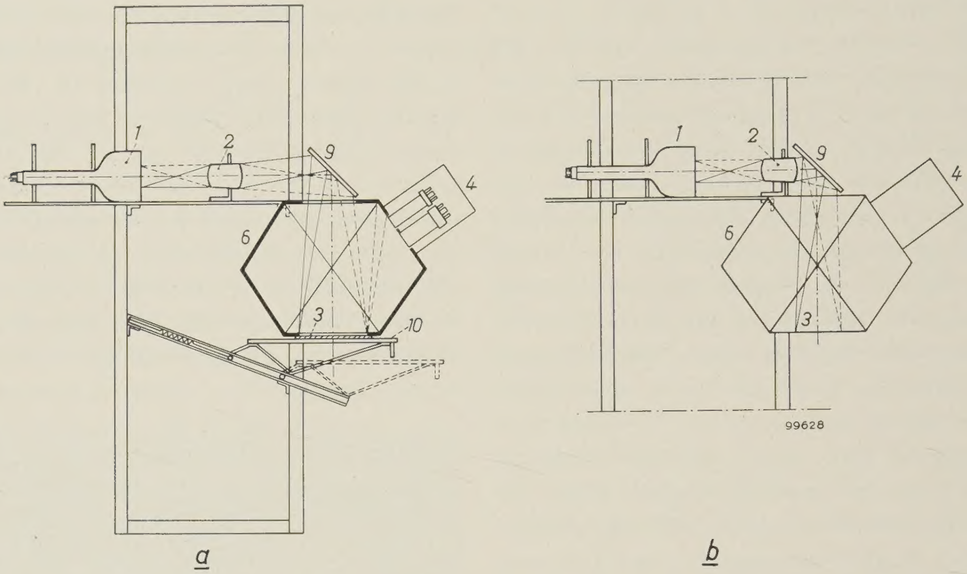

Fig. 24. *a*) Cross-section of the print scanner shown in fig. 23. The figures *1 . . . 9* have the same meaning as in fig. 23. *10* movable platform with the print at position *3*. Scanning tube and objective lens are in position for prints of 18 × 24 cm.
b) Scanning tube and objective lens in position for prints of 11 × 14.5 cm (maximum optical enlargement).

The possibility of enlargement enhances the value of the scanner for use in colour-television broadcasts, since it makes it possible to transmit all manner of coloured prints without faults of register from the signal source.

The spectral sensitivity of the three channels in the print scanner should follow the curves in fig. 8, as in the case of the slide scanner. With the latter this is achieved mainly by the use of dichroic mirrors, additional correction being provided by filters in front of the photocathodes. In the print scanner, however, these mirrors are lacking and the filters are solely responsible for separating the light into the primary colours. It is not an easy matter to find filters capable of meeting the requirements with sufficient accuracy. The solution adopted was to use several different filters, placed side by side over the photomultiplier. If, for example, each half of the photocathode is covered with a different filter, the net spectral transmission is the arithmetical mean of the transmissions of the individual filters. This artifice, which is by no means new, has produced good results.

Summary. In development work on colour television it is desirable that the source of the primary-colour signals should be completely free from errors of register. Colour-television cameras do not meet this requirement, but flying-spot scanners do, and for this reason they have been widely used in colour-television development. Two types have been evolved in the Philips Research Laboratories: one for colour slides and one for opaque matter (colour prints, paintings, coloured drawings, etc. and also small objects.) In both cases the flying spot is produced on the screen of a special cathode-ray tube whose phosphor shows maximum emission at a wavelength of 505 mμ.

In the slide scanner the flying spot is imaged on the transparency by an objective lens, and the objective aperture is imaged on the photocathodes of three photomultiplier tubes (one Philips type 50 AVP, two R.C.A. types 6217) by condenser lenses via dichroic mirrors and correction filters. The video channel of each of the three primary-colour channels has an afterglow compensation section, a gamma correction section and an output amplifier. The latter distributes the colour signals via cables to a test circuit, two monitors and the consumer circuits.

The scanner for colour prints is based on the principle of the integrating-sphere photometer. This provides a light gain of about a factor 7, and also shields the system against extraneous light and reduces vignetting effects. The design and various constructional details of such an experimental print-scanner are discussed.

ABSTRACTS OF RECENT SCIENTIFIC PUBLICATIONS BY THE STAFF OF N.V. PHILIPS' GLOEILAMPENFABRIEKEN

Reprints of these papers not marked with an asterisk * can be obtained free of charge upon application to Philips Electrical Ltd., Century House, Shaftesbury Avenue, London W.C. 2.

2684: F. C. de Ronde: Schwinger's variational principle applied to the calculation of the radiation resistance and radiation reactance of a linear antenna in a waveguide of rectangular cross-section (Commun. Congrès int. Circuits et Antennes Hyperfréquences, Paris 21-26 Oct. 1957, part 1 (suppl. Onde électr. **38**, No. 376 bis), pp. 95-98, 1958).

The radiation impedance of a linear antenna in a waveguide of rectangular cross-section has been calculated on the basis of an assumed sinusoidal antenna current distribution. Because of the rather great discrepancy between theory and experiment a more powerful method is applied to calculate the radiation impedance, viz. Schwinger's variational principle. This new application, even when based on only a two-term Fourier expansion of the current distribution, gives better results than the assumed sinusoidal current distribution.

2685: F. C. de Ronde: A simple component for impedance measurements at cm and mm waves: the direct-reading variable impedance (Commun. Congrès int. Circuits et Antennes Hyperfréquences, Paris 21-26 Oct. 1957, part 1 (suppl. Onde électr. **38**, No. 376 bis), pp. 294-295, 1958).

At cm wavelengths standing-wave indicators are used for impedance measurements. However, it is not simple to make them for mm waves. Impedance measurements can also be done in a bridge. For that reason a variable impedance has been developed which, in combination with a hybrid tee, can be used for impedance measurements. This hybrid tee only has to be symmetrical, so it is not difficult to construct. The modulus and argument of the reflection coefficient of the variable impedance can be adjusted independently of each other. Variable impedances for 3 cm, 8 and 4 mm have been realized. The precision of the modulus of the reflection coefficient is a few percent.

2686: G. Ahsmann and H. J. Oskam: Impedance and recovery time of glow discharges in mixtures of rare gases (J. appl. Phys. **29**, 1768, 1958, No. 12).

Measurements of the impedance of a series of inert gas discharges (13.7 mm Hg, 3.5 mA) by means of a Wagner A.C. bridge, at frequencies of 100 to 15 000 c/s. From these measurements the characteristic quantities, viz. the self-inductance and the differential resistance, are calculated. The results agree well with a theory given by C. van Geel. Additions of a few percent of another inert gas, of lower ionization potential, cause a considerable drop in the modulus of the impedance. An explanation of this effect is given. The influence of the added inert gas on the recovery time will be dealt with in a later publication.

2687: B. Verkerk: Autoradiographic study of the influence of chlorine on semi-conducting alumina layers (Radioisotopes in scientific research, Proc. int. Conf. held in Paris, Sept. 1957, under the auspices of the UNESCO, Pergamon Press, London, New-York and Paris 1958, edited by R. C. Extermann, Vol. 1, pp. 503-515).

The presence of very small quantities of chlorine in the electrolyte has a disastrous effect on the insulating properties of anodically formed alumina layers. An autoradiographic method was used to study the presence and distribution of absorbed chlorine on alumina layers formed in a boric acid bath, to obtain information on the mechanism of this attack. A proposed mechanism attributing the electronic conductance of degenerated layers to a partial displacement of the oxygen in the oxide by chlorine with a corresponding change in the valency of part of the aluminium did not seem to hold in the light of the results obtained. The distributions found pointed toward the presence of imperfections in the oxide layers due to segregations of impurities at isolated places of the aluminium and along grain boundaries of recrystallized samples. Identical distributions were found for some absorbed cations. From this and the work of French investigators it is concluded that the corrosion by chlorine of anodized aluminium is due only to impurities in the metal.

2688: Dutch translation of **2690**.

2689: French translation of **2690**.

2690: H. B. G. Casimir: Certainty in the exact sciences (Koninklijke Nederlandse Akademie van Wetenschappen 1808-1958, N.V. Noord-

Hollandsche Uitgeversmaatschappij, Amsterdam 1958, pp. 243-251).

Philosophic considerations on the certainty that may be attributed to physical theories. Examples from other fields of human endeavour and from the historical development of physical theories are used to illustrate the theme. Even in physics certainty is not absolute: it is limited by the particular assumptions associated with a theory or by the circumstances in which observations are made.

2691: T. Kralt: Ionylamines, III. Catalytic hydrogenation of ionones in the presence of ammonia or amines and the determination of the position of the $> C = C <$ bond in dihydro-α-, dihydro-β- and tetrahydro-ψ-ionylamines (Rec. Trav. chim. Pays-Bas **77**, 990-1003, 1958, No. 11).

The course of the catalytic hydrogenation of ionones in the presence of ammonia or amines has been investigated. In this way it has been possible to determine the position of the remaining $> C = C <$ bond in the dihydro-α-, dihydro-β- and tetrahydro-ψ-ionylamines described previously.

2692: J. H. Uhlenbroek and J. D. Bijloo: Investigations on nematicides, I. Isolation and structure of a nematicidal principle occurring in Tagetes roots (Rec. Trav. chim. Pays-Bas **77**, 1004-1009, 1958, No. 11).

Some highly nematicidal polythienyls have been isolated from the roots of Tagetes plants. One of the compounds was shown to be α-terthienyl.

2693: J. P. L. Bots: Investigations on sterols, XI. Preparation of 13α-androstene derivatives (Rec. Trav. chim. Pays-Bas **77**, 1010-1017, 1958, No. 11).

By irradiation of androst-5-en-3β-ol-17-one with U.V. light ($\lambda > 280$ mμ) 13α-androst-5-en-3β-ol-17-one was obtained. This substance was converted into a mixture of the C_{17} epimers of 13α-androst-4-en-17-ol-3-one, both of which were obtained in a pure state.

2694: F. Brücke, G. Hertting, H. D. Moed and J. van Dijk: Über eine neue Adrenalincarbonsäure und einige ihrer Derivate (Biochem. Pharmacol. **1**, 221-231, 1958). (On a new adrenalin carboxylic acid and some of its derivatives; in German.)

Synthesis and pharmacological properties of a new carboxylic acid of epinephrine and of some derivatives are reported. The carboxylic acid produced qualitatively the same effects on the blood pressure and on the denervated nictitating membrane of the cat as epinephrine, the relative potency being 0.0003. The effects on the blood pressure could be reversed by previous administration of adrenalytics. The authors believe that the effects on the blood pressure and the nictitating membrane are caused by admixture of epinephrine contained in the original substance. An enzymatic decarboxylation in vitro could not be observed. On the other hand, the effects of the esters derived from the new epinephrine carboxylic acid were similar to those of the isopropylnorepinephrine. The most active ester derived from the new acid equalled isopropylnorepinephrine in its potency on all test subjects. In all experiments, the increasing effects on heart frequency, the bronchodilating and the depressing effect on the blood pressure of the esters run parallel. The corresponding derivatives of the p-oxyephedrin were practically completely ineffective. The connections between chemical constitution and pharmacological activity is discussed.

2695: H. G. Beljers: Ferrite isolators in the 8-9 mm wave band (Commun. Congrès int. Circuits et Antennes Hyperfréquences, Paris 21-26 Oct. 1957, part 2 (suppl. Onde électr. **38**, No. 376 ter), pp. 647-648, 1958).

For the construction of isolators at 8-9 mm wavelengths two main principles are applied. The first one is a Faraday rotator type with three ports, which is essentially a circulator. The reflected energy is dissipated in an external load in a waveguide normal to the main guide, decoupled from the input. The second type is a resonance isolator with a transverse magnetic field. The usual soft ferrite samples would require a magnetic field of about 12 000 Oe, which is rather high. If oriented anisotropic materials are applied the required field can be considerably reduced or even omitted. Very simple devices are resultant, although isolation ratios are generally less high than for the normal resonance isolators.